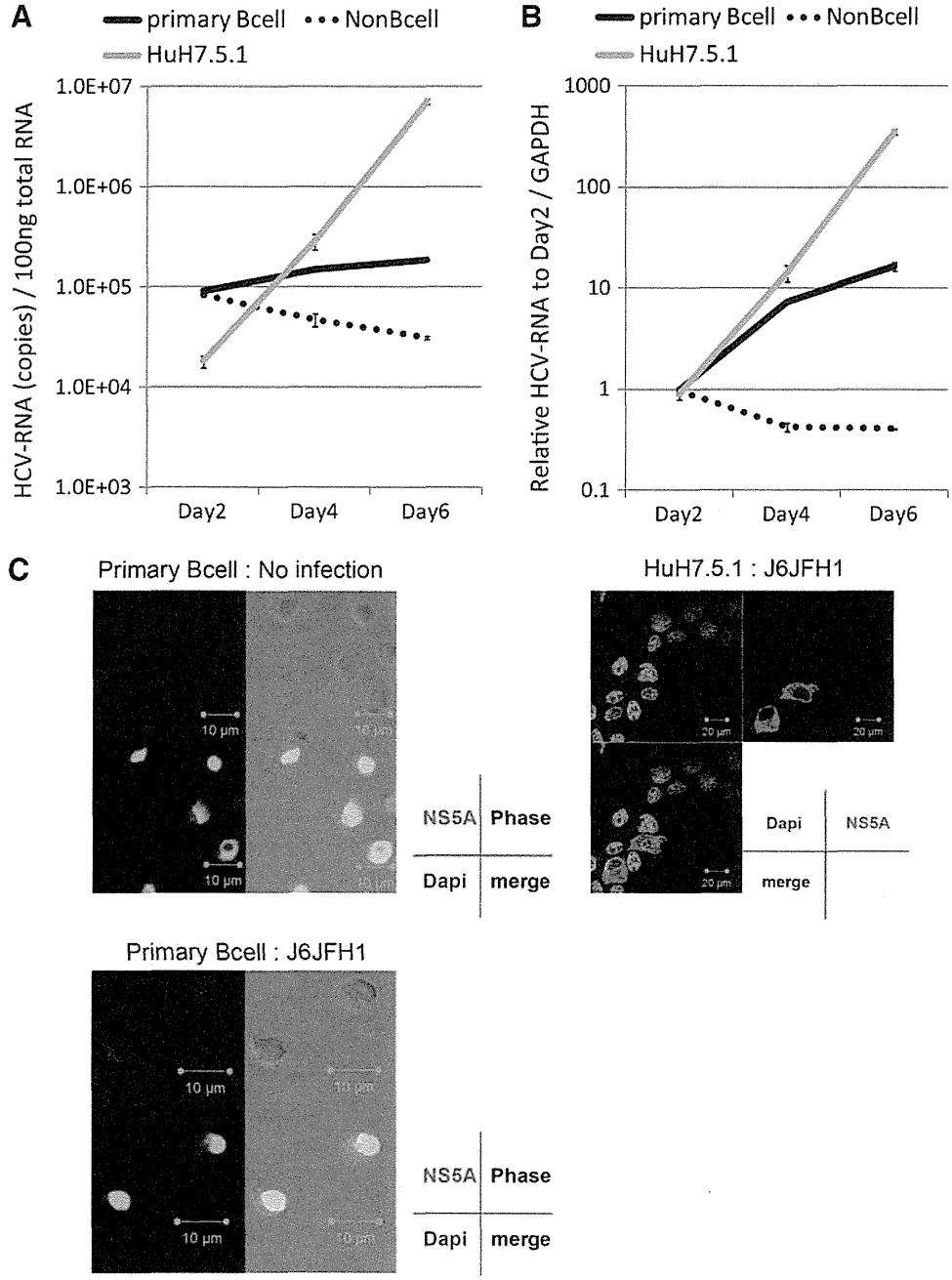


**FIG. 1.** J6JFH1 infects human peripheral blood B-cells. Human B-cells (CD19+ cells) and non-B-cells (CD19− cells) were separated by MACS as described in Materials and Methods. Primary B-cells, non-B-cells, and Huh7.5.1 cells were infected with J6JFH1 at MOI = 1 for 3 h. After infection, cells were washed twice with culture medium and continued culture. On days 2, 4, and 6, total RNA was collected and HCV-derived RNA was determined by reverse transcription polymerase chain reaction (RT-PCR). GAPDH was used as internal control. **(A)** HCV-RNA not adjusted by GAPDH. **(B)** HCV-RNA adjusted by GAPDH. **(C)** Immunofluorescence analysis of J6JFH1-infected human B-cells and Huh7.5.1 cells. Six days postinfection. Red, NS5A; blue: Dapi; phase: phase-shift microscope.

infection, since the negative-strand RNA is not yielded if HCV particles or RNA just adhere to the cell surface of human primary B-cells without internalization (9,14,19,35, 42,43). We measured the synthesis of plus-strand and minus-strand HCV-RNA separately using strand-specific RT primers and rTth polymerase as previously described (4). The titer increase of minus-strand HCV-RNA indicates HCV-RNA replication. As shown in Figure 3, both minus- and plus-strand HCV-RNA increased time dependently in primary B-cells, and both types of RNA concomitantly decreased in non-B-cells (Fig. 3A and B). Plus- and minus-strand RNA were exponentially increased in Huh7.5.1 cells infected with J6JFH1 (Fig. 3C). These results indicated that primary human B-cells supported J6JFH1 infection and replication, although viral replication levels in B-cells were modest compared with those in Huh7.5.1 cells. These results

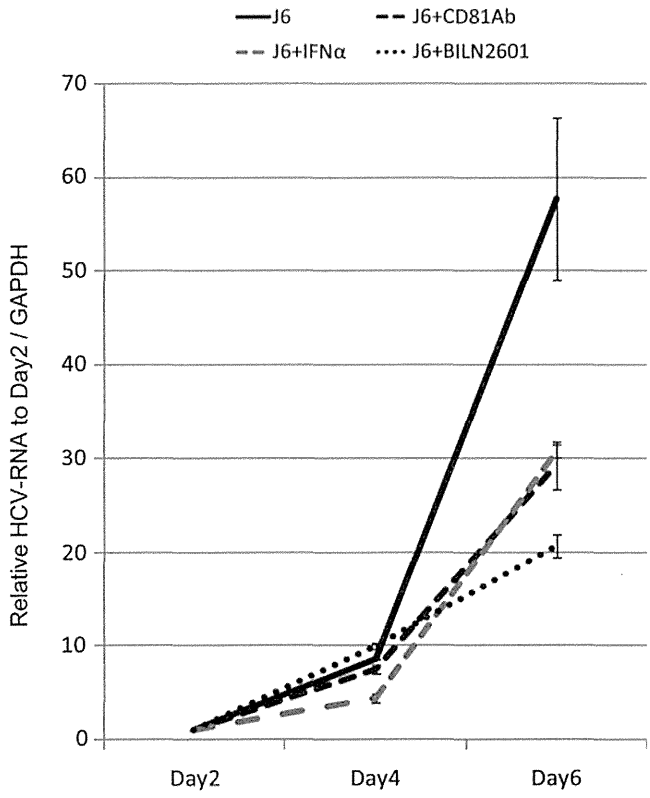


**FIG. 2.** J6JFH1 B-cell infection is blocked by anti-CD81 Ab, IFN-α, or an NS3/4A inhibitor. Anti-CD81 neutralizing Ab (20 μg/mL) was added to the B-cell culture 1 h before infection. Otherwise, recombinant IFN-α rhIFN-α, 200 IU/mL) or BLIN2601 (250 nM, which is IC75; see Supplementary Fig. S3) was added 1 h after infection. On days 2, 4, and 6, total RNA was extracted, and HCV-RNA was determined by RT-PCR. The values were adjusted by GAPDH.

may reflect the fact that the NS5A protein is difficult to detect in infected B-cells using IF assay.

### *B-cells can be infected with different HCV strains*

We next used the Jc1/GLuc2A strain to investigate whether different HCV strains infect primary B-cells. Primary B-cells, non-B-cells (data not shown), and Huh7.5.1 cells were infected with the Jc1/GLuc2A strain. After five washes, supernatant was collected (day 0 samples). On days 2, 4, and 6, medium was collected. Luciferase activity was determined for all samples by luminescence (GLuc). GLuc activity and detection of RNA increased exponentially in Huh7.5.1 cells infected with the Jc1/GLuc2A strain (Fig. 4A). GLuc activity on day 4 to day 6 increased more in primary B-cells than in non-B-cells (Fig. 4B). These results suggest that HCV replication is substantial, but low in the HCV line Jc1/GLuc2A.

### *B-cells neither produce nor release detectable level of HCV infectious particles*

We collected supernatants of J6JFH1-infected primary human B-cells to measure productive infection in B-cells. The supernatant was then added to culture of Huh7.5.1 cells, and we compared infection with control Huh7.5.1 cells, whose cells were infected with a low MOI (0.01 and 0.001) of J6JFH1 collected from media of the infected Huh7.5.1 cells. HCV-RNA titer in the Huh7.5.1 titrating cells was decreased over time after co-culture with B-cell supernatants obtained from either "releasing samples" "assembly samples." In contrast, HCV-RNA titers were slightly increased over time in the Huh7.5.1 titrating cells that had been infected with medium collected from low MOI-J6JFH1-infected Huh7.5.1 cells (Fig. 5). These results indicated that primary human B-cells were infected with J6JFH1 but failed to assemble or produce particles into the supernatant.

### *Host response to HCV infection into primary B-cells*

Next, we determined whether B-cell activation was induced in HCV-infected B-cells that survived under HCV infection. We measured induction of CD80 and CD86 as B-cell activation markers. After 2–3 days of infection, the CD80/86 levels on B-cells treated with J6JFH1 were compared with those treated with medium from mock-infected cells (concentrated Huh7.5.1 medium) by FACS analysis (Fig. 6A). We found that CD80/86 were upregulated in infected cells compared to mock-infected cells.

Since B-cell lymphoma is a known complication of chronic HCV infection (20,36) and acquiring apoptotic resistance is essential for the development of cancer (21,51,38), we measured the ability of B-cells to escape apoptosis after HCV infection. B-cell apoptosis spontaneously occurs during culture at 37°C. The percent of apoptosis of primary B-cells was decreased in FACS analysis using 7AAD viaprobe + annexinV (Fig. 6B) and ATP assays postinfection (Fig. 6C). These results suggest that primary B-cells are protected from apoptosis by infection with HCVcc. It has been reported that B-cells were vulnerable to apoptotic cell death at various stages of peripheral differentiation and during signal responses (18). Thus, the results infer that HCV stimulation interferes with B-cell apoptotic signal in human B-cells.

## Discussion

We show evidence suggesting that human peripheral B-cells can be infected with HCV strains. Establishment of J6JFH1 infection was evaluated by minus-strand PCR amplification, production of core and NS5A proteins, and protection from apoptosis. An increase in HCV RNA in B-cells was inhibited by an exogenously added antibody against CD81 that blocked HCV receptor function. Furthermore, blocking HCV replication in B-cells by type I IFN and NS3/4A protease inhibitor confirmed the presence of HCV infection/replication in human B-cells. The results were corroborated with another HCV strain, Jc1/GLuc2A. Although we failed to establish an EBV-transformed B-cell line to reproduce HCV infection of B-cells, peripheral blood B-cells were infected with J6JFH1 in 12 independent experiments.

One of the well-known complications of chronic HCV infection is LPD, including cryoglobulinemia and B-cell malignant lymphoma, indicating the involvement of B-cells in the course of the disease (1,12,15,16). However, many reports describing the existence of the HCV genome in B-cells and lymphomas (21,25,51) and HCV replication in B-cells have been controversial due to multiple artifacts complicated in detection and quantitation of the replicative

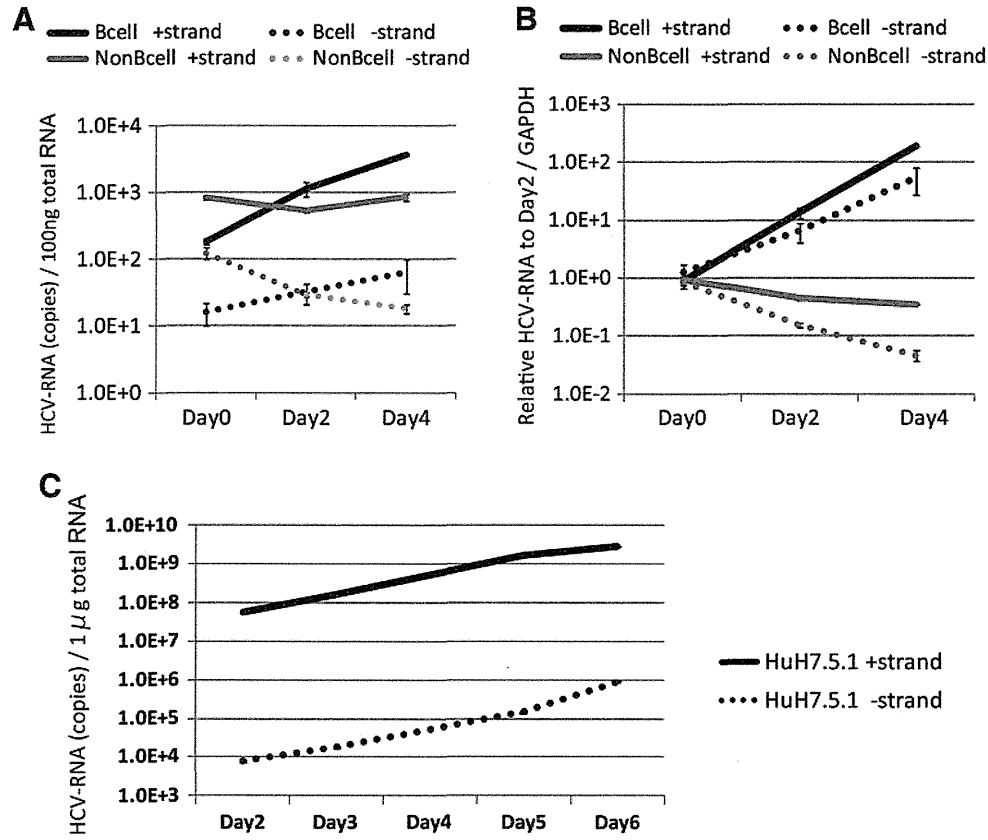


**FIG. 3.** HCV negative strand RNA is detected in human B-cells. By using rTth methods, HCV strand-specific RNA was determined in J6JFH1-infected human B-cells. **(A)** Not only plus strand HCV-RNA but also minus strand HCV-RNA were increased in a time-dependent manner in human B-cells. **(B)** When HCV-RNA was adjusted by GAPDH that was used as an internal control, HCV-RNAs in B-cells were substantially increased compared with those in non-B-cells. **(C)** Plus and minus strand HCV-RNAs were efficiently amplified in J6JFH1-infected Huh 7.5.1 cells. The level of HCV-RNA exponentially increased in this hepatocyte line.

intermediate minus strand RNA (29,31). This has led to a continuous debate about HCV infection in B-lymphocytes.

HCV entry into B-cells has also been previously reported to be absent because retroviral (37) and lentiviral (8) pseudoparticles bearing HCV envelope glycoproteins (HCVpp) did not infect primary B-cells or B-cell lines. In our study, while we succeeded in infecting Huh7.5.1 cells efficiently with retroviral pseudoparticles for expressing both HCV E1/E2 and the control VSV-G, we failed to establish the same infection in B-cells, suggesting that the block of pseudoparticle entry into B-cells is not related to HCV glycoproteins alone.

Total PBMCs reportedly facilitate HCV attachment but not internalization (42), so HCV infection of B-cells is abrogated in total PBMCs (35). The cause of HCV absorption is unclear, but incomplete sets of HCV receptors in non-B PBMC cells permit attachment of HCV without internalization. B-cells possess CD81, SRBI, LDL-R, and NPC1L1. Because B-cells are not adherent cells, they do not express claudin 1 and occludin, which forms a receptor complex for HCV (9,14,19,43). Claudin 1 and occludin are components of tight junctions and serve as HCV receptors in human hepatocytes. In infection studies using cells expressing these proteins, however, claudin 1 and occludin only upgrade infection efficacy and are dispensable to infection (5), although CD81 is essential for establishment of infection (42). Lack of claudin 1 and occludin or miR122 might be a cause of the low HCV infection efficiency observed in human B-cells. Function blocking of CD81 by its specific antibody suppressed HCV infection in primary B-lymphocytes, which imply that HCV entry into primary B-lymphocyte is dependent on the direct interaction phenomenon between HCV virus particles and CD81 receptor and is not mediated by other nonspecific (CD81 independent) pathways such as exosomal transfer of HCV from Huh7 cells to nonhepatic cells, such as dendritic cells (46).

Previous report using *in vitro* prepared recombinant HCV JFH1 particles (HCVcc) failed to establish HCV infection in B-lymphocyte cell lines (39). While HCV is known to infect human hepatocytes *in vivo* leading to chronic viral hepatitis, in the *in vitro* conditions, only the combination between Huh7 cells and its derived clones supported robust replication and infection with only JFH1 or its derived chimeras (5). Neither hepatocyte cell lines including primary hepatocytes nor other HCV strains could reproduce HCV infection efficiently *in vitro* (5). These data suggest that the clonal selection of HCV quasispecies by hepatoma Huh7 cells is essential for this robust infection *in vitro*. The situation would be similar to the JFH1 story in B-cell HCV infection.

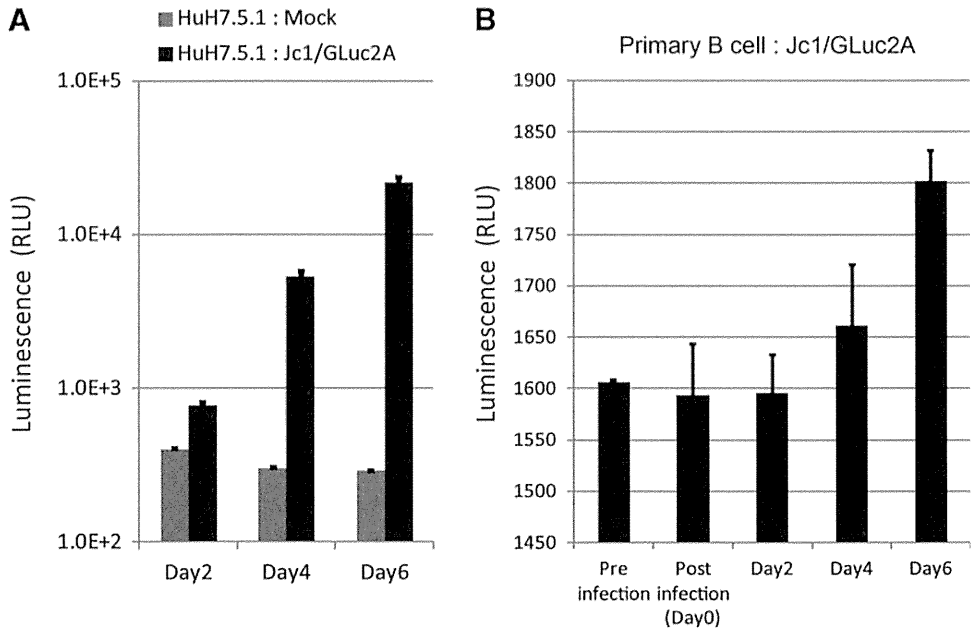


**FIG. 4.** Jc1/GLuc2A strain infects human B-cells with an increase of Gluc activity. Human B-cells and Huh7.5.1 cells were infected with the JC1/GLuc2A strain that contains secretory luciferase derived from *Gaussia* (GLuc) at MOI = 5. Huh7.5.1 cells were used as control. GLuc activity was increased as time cultured. The GLuc activity was saturated in Huh7.5.1 (**A**). On the other hand, GLuc activity was increased from day 4 in human B-cells (**B**).

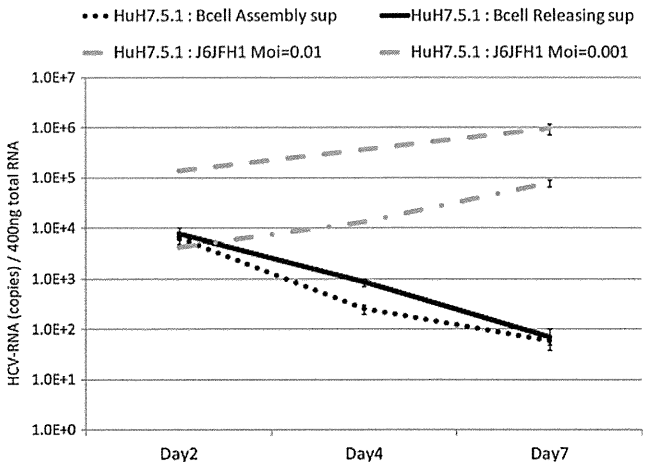


**FIG. 5.** B-cells infected with J6JFH1 fail to produce virus particles. Human B-cells were infected with J6JFH1 for 3 h, washed twice with phosphate buffered saline (PBS), and cultured. Six days after infection, the supernatant was collected ("releasing samples"). Cells were periodically frozen and thawed five times, and the supernatant was collected ("assembly samples"). For evaluation of the infectious virions, Huh7.5.1 cells were treated with these "releasing samples" or "assembly samples." Similarly, Huh7.5.1 cells were treated with J6JFH1 at low MOI (MOI = 0.01 and 0.001) in parallel. After the treatment, cells were washed and cultured. On days 2, 4, and 7, cells were harvested to collect HCV-RNA. Total RNA was extracted from each samples, and HCV-RNA was determined by RT-PCR methods.

B-cell apoptosis spontaneously occurs during culture at 37°C. We found that B-cell apoptosis was blocked by J6JFH1 infection, as reported previously using Raji cells (11). B-cell apoptosis usually occurs secondary to viral infection, but HCV is particular since apoptotic signaling interferes with infection, leading to protection from cell death. However, B-cell survival was not due to primary infection, because the percent of cells circumventing apoptosis was usually higher than cells infected with HCV. We could not define the pathways that participated in apoptosis regulation by HCV, although a previous report (11) suggested that E2-CD81 engagement was related to B-lymphocyte disorders and weak neutralizing antibody response in HCV patients. Since B-cell lymphoma is a known complication of chronic HCV infection (27), the inability of infected cells to undergo apoptosis can be associated with the development of cancer (28,33,49). In this context, B-cell lymphoma often occurs in mice with Cre-initiated HCV transgenes (26). It is notable that anti-apoptotic effect of HCV core gene was reported in genotype 3a in Huh7 cells (23) and, here, genotype 2a in B-cells. In another report (51), HCV strains established from B-cell lymphoma persistently infected with HCV were genotype 2b. B-cell HCV infection might not be linked to some specific genotypes of HCV.

We believe that our report shows that human primary B-cells can be infected *in vitro* with HCV, and that this infection is dependent on HCV particles binding with its receptor CD81 and is not nonspecific entry (e.g., exosomal mediated). We also show that this infection could be blocked with antibodies interfering with this binding, or with drugs that suppress HCV replication. Although no virion was generated from B-cells in HCV infection, it is still likely that B-cells serve as a temporal reservoir of HCV in the blood circulation. If B-cells permit HCV infection, RNA sensors

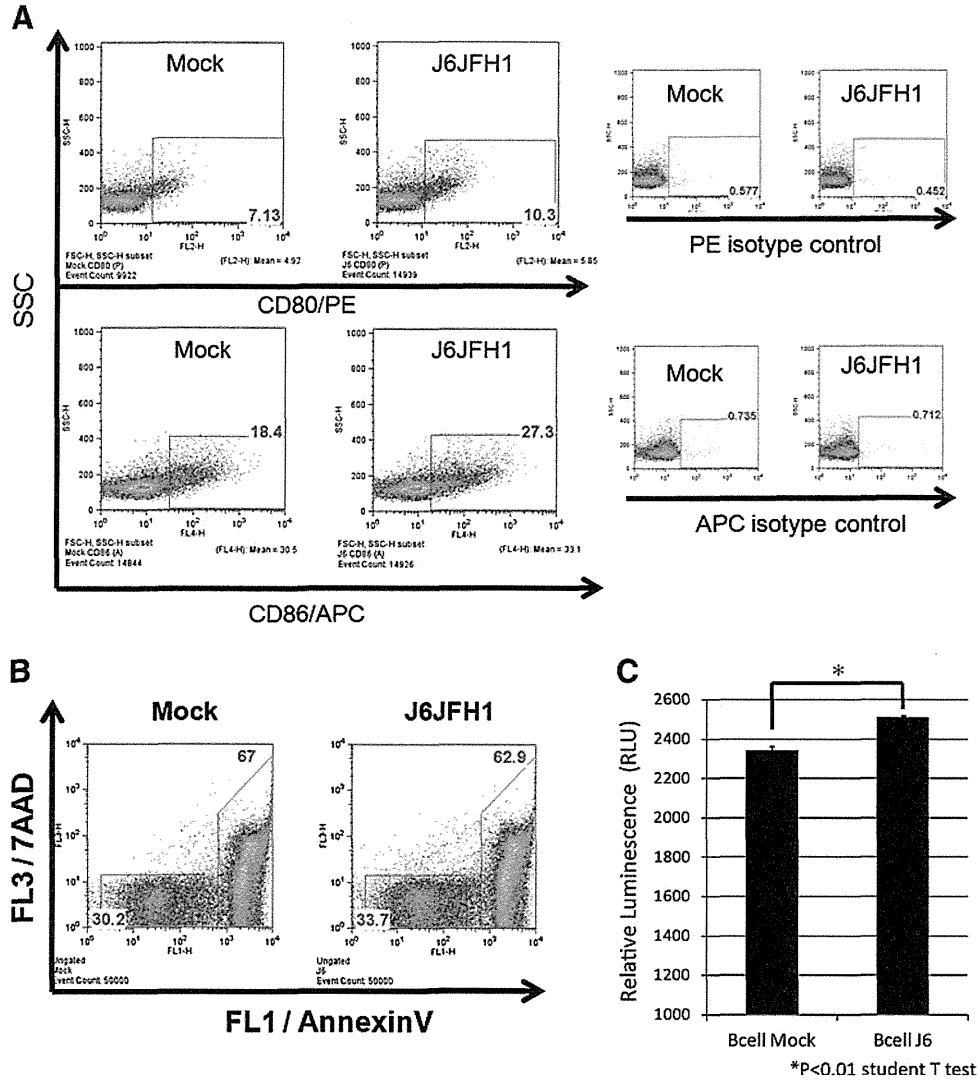


**FIG. 6.** J6JFH1 infection activates B-cells and protects the cells from apoptosis. Human B-cells were infected with J6JFH1 at MOI = 1 for 3 h, washed twice with PBS, and cultured. Two days after inoculation, cells were washed and suspended with FACS buffer. **(A)** The cells were incubated with PE-conjugated anti-human CD80 antibody, APC-conjugated CD86 antibody, or PE/APC-conjugated mouse IgG1 isotype control for 30 min. Then, the cells were washed and resuspended in FACS buffer. Cells were analyzed by FACS. **(B)** Annexin V and 7AAD viaprobe were added and cultured at 18°C for 10 min. Then, cells were analyzed by FACS. **(C)** $2 \times 10^5$ human B-cells were infected with J6JFH1- or Mock-concentrated medium for 3 h. Cells were then washed, resuspended, and cultured in a 96-well white microwell plate. Two days later, ATP activity was determined with a CellTiter-Glo® Luminescent Cell Viability Assay Kit (Promega). ATP activity was adjusted by day 0 ATP activity.

RIG-I and MDA5 in B-cells might recognize HCV RNA and evoke intracellular signaling, including by transcription factors NF-κB and IRF-3/7 (5). Activation of the cytokine network is triggered in human B-cells in response to HCV RNA. In fact, host factors liberated by HCV-infecting B-cells have been previously reported in HCV patients (1,12,15,16,52). Although patients' outcomes would be more than we can be predicted from our results, this system would actually benefit the future study on B-cell–virus interaction.


## Acknowledgments

We are grateful to Drs. Frank Chisari (Scripps Research Institute, San Diego, CA) for the Huh7.5.1 cells, Takaji Wakita (National Institute of Infectious Diseases, Tokyo) for supplying the J6JFH1 plasmid, and Brett Lindenbach (Yale University, New Haven, CT) for providing us with the pJc1-GLuc2A HCV strain.

This work was supported in part by Grants-in-Aid from the Ministry of Education, Science, and Culture (Specified Project for "Carcinogenic Spiral") and the Ministry of Health, Labor, and Welfare of Japan, and by the Program of Founding Research Centers for Emerging and Reemerging Infectious Diseases, MEXT. Financial support by the Takeda Science Foundation, the Yasuda Cancer Research Foundation, and the Iskra Foundation are gratefully acknowledged.


## Author Disclosure Statement

No competing financial interests exist.

## References


1. Agnello V, Chung RT, and Kaplan LM. A role for hepatitis C virus infection in type II cryoglobulinemia. N Engl J Med 1992;327:1490–1495.
2. Aizaki H, Morikawa K, Fukasawa M, *et al.* Critical role of virion-associated cholesterol and sphingolipid in hepatitis C virus infection. J Virol 2008;82:5715–5724.
3. Aly HH, Oshiumi H, Shime H, *et al.* Development of mouse hepatocyte lines permissive for hepatitis C virus (HCV). PLoS One 2011;6:e21284.
4. Aly HH, Qi Y, Atsuzawa K, *et al.* Strain-dependent viral dynamics and virus–cell interactions in a novel *in vitro* system supporting the life cycle of blood-borne hepatitis C virus. Hepatology 2009;50:689–696.
5. Aly HH, Shimotohno K, Hijikata M, and Seya T. *In vitro* models for analysis of the hepatitis C virus life cycle. Microbiol Immunol 2012;56:1–9.
6. Asselah T, and Marcellin P. Second-wave IFN-based triple therapy for HCV genotype 1 infection: simeprevir, faldaprevir and sofosbuvir. Liver Int 2014;34:60–68.
7. Bare P, Massud I, Parodi C, *et al.* Continuous release of hepatitis C virus (HCV) by peripheral blood mononuclear cells and B-lymphoblastoid cell-line cultures derived from HCV-infected patients. J Gen Virol 2005;86:1717–1727.
8. Bartosch B, Dubuisson J, and Cosset FL. Infectious hepatitis C virus pseudo-particles containing functional E1-E2 envelope protein complexes. J Exp Med 2003;197; 633–642.
9. Bartosch B, Vitelli A, Granier C, *et al.* Cell entry of hepatitis C virus requires a set of co-receptors that include the CD81 tetraspanin and the SR-B1 scavenger receptor. J Biol Chem 2003;278:41624–41630.
10. Castet V, Fournier C, Soulier A, *et al.* Alpha interferon inhibits hepatitis C virus replication in primary human hepatocytes infected *in vitro*. J Virol 2002;76:8189–8199.
11. Chen Z, Zhu Y, Ren Y, *et al.* Hepatitis C virus protects human B lymphocytes from Fas-mediated apoptosis via E2-CD81 engagement. PLoS One 2011;6:e18933.
12. Donada C, Crucitti A, Donadon V, *et al.* Systemic manifestations and liver disease in patients with chronic hepatitis C and type II or III mixed cryoglobulinaemia. J Viral Hepat 1998;5:179–185.
13. Ebihara T, Shingai M, Matsumoto M, Wakita T, and Seya T. Hepatitis C virus-infected hepatocytes extrinsically modulate dendritic cell maturation to activate T cells and natural killer cells. Hepatology 2008;48:48–58.
14. Evans MJ, von Hahn T, Tscherne DM, *et al.* Claudin-1 is a hepatitis C virus co-receptor required for a late step in entry. Nature 2007;446:801–805.
15. Ferri C, Caracciolo F, Zignego AL, *et al.* Hepatitis C virus infection in patients with non-Hodgkin's lymphoma. Br J Haematol 1994;88:392–394.
16. Frangeul L, Musset L, Cresta P, Cacoub P, Huraux JM, and Lunel F. Hepatitis C virus genotypes and subtypes in patients with hepatitis C, with and without cryoglobulinemia. J Hepatol 1996;25:427–432.
17. Fried MW, Buti M, Dore GJ, *et al.* Once-daily simeprevir (TMC435) with Pegylated interferon and ribavirin in treatment-naïve genotype 1 hepatitis C: the randomized PILLAR Study. Hepatology 2013;58:1918–1929.
18. Harwood NE, and Batista FD. New insights into the early molecular events underlying B cell activation. Immunity 2008;28:609–619.
19. Hsu M, Zhang J, Flint M, *et al.* Hepatitis C virus glycoproteins mediate pH-dependent cell entry of pseudotyped retroviral particles. Proc Natl Acad Sci U S A 2003;100: 7271–7276.
20. Inokuchi M, Ito T, Uchikoshi M, *et al.* Infection of B cells with hepatitis C virus for the development of lymphoproliferative disorders in patients with chronic hepatitis C. J Med Virol 2009;627:619–627.
21. Ito M, Masumi A, Mochida K, *et al.* Peripheral B cells may serve as a reservoir for persistent hepatitis C virus infection. J Innate Immun 2010;2:607–617.
22. Jacobson IM, McHutchison JG, Dusheiko G, *et al.* Telaprevir for previously untreated chronic hepatitis C virus infection. N Engl J Med 2011;364:2405–2416.
23. Jahan S, Khaliq S, Siddiqi MH, *et al.* Anti-apoptotic effect of HCV core gene of genotype 3a in Huh-7 cell line. Virol J 2011;8:522.
24. Kambara H, Fukuhara T, Shiokawa M, *et al.* Establishment of a novel permissive cell line for the propagation of hepatitis C virus by expression of microRNA miR122. J Virol 2012;86:1382–1393.
25. Karavattathayyil SJ, Kalkeri G, Liu HJ, *et al.* Detection of hepatitis C virus RNA sequences in B-cell non-Hodgkin lymphoma. Am J Clin Pathol 2000;113:391–398.
26. Kasama Y, Sekiguchi S, Saito M, *et al.* Persistent expression of the full genome of hepatitis C virus in B cells induces spontaneous development of B-cell lymphomas *in vivo*. Blood 2010;116;4926–4933.
27. Kondo Y, and Shimosegawa T. Direct effects of hepatitis C virus on the lymphoid cells. World J Gastroenterol 2013; 19:7889–7895.
28. Ladu S, Calvisi DF, Conner EA, Farina M, Factor VM, and Thorgeirsson SS. E2F1 inhibits c-Myc-driven apoptosis via PIK3CA/Akt/mTOR and COX-2 in a mouse model of human liver cancer. Gastroenterology 2008;135:1322–1332.
29. Lanford RE, Chavez D, Chisari FV, and Sureau C. Lack of detection of negative-strand hepatitis C virus RNA in peripheral blood mononuclear cells and other extrahepatic tissues by the highly strand-specific rTth reverse transcriptase PCR. J Virol 1995;69:8079–8083.
30. Laskus T, Radkowski M, Wang LF, Vargas H, and Rakela J. The presence of active hepatitis C virus replication in lymphoid tissue in patients coinfected with human immunodeficiency virus type 1. J Infect Dis 1998;178:1189–1192.
31. Lerat H, Berby F, Trabaud MA, *et al.* Specific detection of hepatitis C virus minus strand RNA in hematopoietic cells. J Clin Invest 1996;97:845–851.
32. Lok AS, Gardiner DF, Hézode C, *et al.* Randomized trial of daclatasvir and asunaprevir with or without PegIFN/RBV for hepatitis C virus genotype 1 null responders. J Hepatrol 2014;60:490–499.
33. Lowe SW, and Lin AW. Apoptosis in cancer. Carcinogenesis 2000;21:485–495.
34. MacParland SA, Pham TN, Guy CS, and Michalak TI. Hepatitis C virus persisting after clinically apparent sustained virological response to antiviral therapy retains infectivity *in vitro*. Hepatology 2009;49:1431–1441.
35. Marukian S, Jones CT, Andrus L, *et al.* Cell culture-produced hepatitis C virus does not infect peripheral blood mononuclear cells. Hepatology 2008;48:1843–1850.
36. Mazzaro C, Franzin F, Tulissi P, *et al.* Regression of monoclonal B-cell expansion in patients affected by mixed cryoglobulinemia responsive to alpha-interferon therapy. Cancer 1996;77:2604–2613.

37. McKeating JA, Zhang LQ, Logvinoff C, *et al.* Diverse hepatitis C virus glycoproteins mediate viral infection in a CD81-dependent manner. J Virol 2004;78:8496–8505.
38. Mizuochi T, Ito M, Takai K, and Yamaguchi K. Peripheral blood memory B cells are resistant to apoptosis in chronic hepatitis C patients. Virus Res 2011;155:349–351.
39. Murakami K, Kimura T, Shoji I, *et al.* Virological characterization of the hepatitis C virus JFH-1 strain in lymphocytic cell lines. J Gen Virol 2008;89:1587–1592.
40. Muratori L, Gibellini D, Lenzi M, *et al.* Quantification of hepatitis C virus-infected peripheral blood mononuclear cells by *in situ* reverse transcriptase-polymerase chain reaction. Blood 1996;88:2768–2774.
41. Phan T, Beran RKF, Peters C, Lorenz IC, and Lindenbach BD. Hepatitis C virus NS2 protein contributes to virus particle assembly via opposing epistatic interactions with the E1-E2 glycoprotein and NS3-NS4A enzyme complexes. J Virol 2009;83:8379–8395.
42. Pileri P, Uematsu Y, Campagnoli S, *et al.* Binding of hepatitis C virus to CD81. Science 1998;282:938–941.
43. Ploss A, Evans MJ, Gaysinskaya VA, *et al.* Human occludin is a hepatitis C virus entry factor required for infection of mouse cells. Nature 2009;457:882–886.
44. Qu J, Zhang Q, Li Y, *et al.* The Tat protein of human immunodeficiency virus-1 enhances hepatitis C virus replication through interferon gamma-inducible protein-10. BMC Immunol 2012;13:15.
45. Radkowski M, Gallegos-Orozco JF, Jablonska J, *et al.* Persistence of hepatitis C virus in patients successfully treated for chronic hepatitis C. Hepatology 2005;41:106–114.
46. Ramakrishnaiah V, Thumann C, Fofana I, *et al.* Exosome-mediated transmission of hepatitis C virus between human hepatoma Huh7.5 cells. Proc Natl Acad Sci U S A 2013; 110:13109–13113.
47. Sarhan MA, Pham TNQ, Chen AY, and Michalak TI. Hepatitis C virus infection of human T lymphocytes is mediated by CD5. J Virol 2012;86:3723–3735.
48. Schmidt WN, Stapleton JT, LaBrecque DR, *et al.* Hepatitis C virus (HCV) infection and cryoglobulinemia: analysis of whole blood and plasma HCV RNA concentrations and correlation with liver histology. Hepatology 2000;31: 737–744.
49. Schulze-Bergkamen H, Krammer P.H. Apoptosis in cancer—implications for therapy. Semin Oncol 2004;31: 90–119.
50. Seto WK, Lai CL, Fung J, *et al.* Natural history of chronic hepatitis C: genotype 1 versus genotype 6. J Hepatol 2010; 53:444–448.
51. Sung VM, Shimodaira S, Doughty AL, *et al.* Establishment of B-cell lymphoma cell lines persistently infected with hepatitis C virus *in vivo* and *in vitro*: the apoptotic effects of virus infection. J Virol 2003;77:2134–2146.
52. Turner NC. Hepatitis C and B-cell lymphoma. Ann Oncol 2003;14:1341–1345.
53. Wakita T, Pietschmann T, Kato T, *et al.* Production of infectious hepatitis C virus in tissue culture from a cloned viral genome. Nature Med 2005;11:791–796.

Address correspondence to:
*Dr. Tsukasa Seya*
*Department of Microbiology and Immunology*
*Hokkaido University Graduate School of Medicine*
*Kita 15, Nishi 7*
*Kita-ku*
*Sapporo 060-8638*
*Japan*

*E-mail:* seya-tu@pop.med.hokudai.ac.jp

JOURNAL OF INTERFERON & CYTOKINE RESEARCH
Volume 00, Number 00, 2014

DOI: 10.1089/jir.2014.0113

**FULL MANUSCRIPT**

# Murine Herc6 Plays a Critical Role in Protein ISGylation *In Vivo* and Has an ISGylation-Independent Function in Seminal Vesicles

Kei-ichiro Arimoto,[1] Takayuki Hishiki,[2] Hiroshi Kiyonari,[3] Takaya Abe,[3] Chuyi Cheng,[4] Ming Yan,[1] Jun-Bao Fan,[1] Mitsuru Futakuchi,[5] Hiroyuki Tsuda,[6] Yoshiki Murakami,[7] Hideyuki Suzuki,[8] Dong-Er Zhang,[1,9] and Kunitada Shimotohno[10]

ISG15 conjugation (ISGylation) to proteins is a multistep process involving interferon (IFN)-inducible UBE1L (E1), UbcH8 (E2), and ISG15 E3 ligases (E3s). Studies performed over the past several years have shown that ISGylation plays a pivotal role in the host antiviral response against certain viruses. Recent *in vitro* studies revealed that human Herc5 and mouse Herc6 are major ISG15 E3 ligases, respectively. However, the global function of Herc5/6 proteins *in vivo* still remains unclear. Here, we report generation and initial characterization of Herc6 knockout mice. Substantial reductions of ISGylation were observed in Herc6-deficient cells after polyinosinic-polycytidylic acid double-stranded RNA injection of mice or IFN treatment of cells. On the other hand, Herc6-deficient cells and wild-type (WT) cells had similar responses to IFN stimulation, Sendai virus (Z strain) infection, and vesicular stomatitis virus infection. These results indicate that Herc6 does not play a critical role in antiviral defense of these viral infections in mice. Interestingly, male Herc6-deficient mice showed seminal vesicle hypertrophy. No such problem was detected in WT and ISG15 activating enzyme Ube1L-deficient mice. These results suggest that in addition to promoting protein ISGylation, Herc6 has a novel and protein ISGylation-independent function in the male reproductive system.

## Introduction

ISG15 is a 17 kDa ubiquitin-like modifier. Its expression is rapidly induced by type I interferon (IFN) (Bedford and others 2011). Similar to ubiquitin, ISG15 is conjugated to lysines on broad target proteins through the reaction of specific E1-activating (UBE1L), E2-conjugating (UbcH8), and E3-ligase enzymes (Yuan and Krug 2001; Kim and others 2004; Dastur and others 2006; Wong and others 2006). The deconjugation of ISG15 from cellular proteins is carried out by USP18 (Burkart and others 2013). Previous *in vitro* knockdown studies suggested that human Herc5 and mouse Herc6 are the main ISG15 E3 ligases to mediate global conjugation in human cells and mouse cells, respectively (Wong and others 2006; Oudshoorn and others 2012). Mice do not possess the Herc5 gene among the Herc family genes. Human Herc6, which is the closest relative to human Herc5, was devoid of any ISG15 E3 ligase activity (Hochrainer and others 2005; Dastur and others 2006; Oudshoorn and others 2012).

ISG15-mediated antiviral activity against influenza, herpes, and Sindbis virus has been shown *in vivo* by means of infections in ISG15$^{-/-}$ and UBE1L$^{-/-}$ mice (Lenschow and others 2005, 2007; Lai and others 2009; Lenschow 2010). In addition, *in vitro* studies for either the overexpression of ISG15 or knockdown of ISG15 using siRNA have implicated ISGylation in the regulation of influenza B virus, vaccinia virus, Sindbis virus, herpes simplex-1 virus, Sendai virus, and Japanese

[1]Moores UCSD Cancer Center, University of California, San Diego, La Jolla, California.
[2]Laboratory of Primate Model, Experimental Research Center for Infectious Diseases, Institute for Virus Research, Kyoto University, Sakyo-ku, Kyoto, Japan.
[3]Laboratory for Animal Resources and Genetic Engineering, RIKEN Center for Developmental Biology (CDB), Kobe, Hyogo, Japan.
[4]Division of Biological Sciences, University of California, San Diego, La Jolla, California.
[5]Department of Molecular Toxicology, Graduate School of Medical Sciences, Nagoya City University, Nagoya, Aichi, Japan.
[6]Laboratory of Nanotoxicology Project, Nagoya City University, Nagoya, Aichi, Japan.
[7]Department of Hepatology, Graduate School of Medicine, Osaka City University, Osaka-shi, Osaka, Japan.
[8]Oriental Bio Service, Inc., Kobe BM Laboratory, Kobe-shi, Hyogo, Japan.
[9]Department of Pathology, University of California, San Diego, La Jolla, California.
[10]Research Center for Hepatitis and Immunology, National Center for Global Health and Medicine, Ichikawa-shi, Chiba, Japan.

encephalitis virus, as well as in the release of virus-like particles derived from HIV-1 and avian sarcoma leukosis virus (Okumura and others 2006, 2008; Guerra and others 2008; Malakhova and Zhang 2008; Hsiang and others 2009; Hsiao and others 2010; Lenschow 2010; Pincetic and others 2010). Although the mechanism by which ISG15 is regulating viral growth is still unknown for the majority of these viruses, it has been reported that ISG15 achieves its antiviral role by conjugating to target proteins, including both host proteins and viral proteins, and altering their functions. For example, ISG15 can be conjugated to host antiviral protein interferon regulatory factor 3 (IRF3) and, thus, stabilize IRF3 by inhibiting its interaction with peptidyl-prolyl cis-trans isomerase NIMA-interacting 1 (PIN1), a protein that promotes IRF3 ubiquitination and degradation (Shi and others 2010). In most overexpression studies, ISG15 and its conjugation-related enzymes have been coexpressed, suggesting that ISG15 conjugation to target proteins is required for these antiviral effects. Despite these observations with either *in vivo* or *in vitro* studies, there are some controversial phenotypes: No differences in viral growth of influenza A, herpes simplex virus-1, Sindbis, and wild-type (WT) vaccinia virus in ISG15$^{-/-}$ mouse embryonic fibroblast cells (MEFs) and vesicular stomatitis virus (VSV) in UBE1L$^{-/-}$ MEFs have also been reported (Osiak and others 2005; Kim and others 2006; Lenschow and others 2007; Guerra and others 2008).

A recent report indicated that human Herc5 globally targets *de novo* synthesized proteins for ISG15 conjugation, thereby making viral proteins major targets for ISGylation (Durfee and others 2010). However, the question remains whether Herc5 and global ISGylation are important for antiviral activity *in vivo*, as ISGylation-mediated antiviral effects might be due to other minor ISG15 E3 ligases with more narrow specificity, such as estrogen-responsive finger protein (EFP, also called TRIM25) (Park and others 2014). Since there is no mouse ortholog of human HERC5, the other members of HERC family proteins have been examined for ISG15 E3 activity. A recent report shows that Herc6 knockdown in mouse L929 cells abolished global ISGylation, whereas its overexpression enhanced ISGylation as well as IFN-β production, and conferred antiviral activity against vesicular stomatitis virus and Newcastle disease virus, which indicated that Herc6 is likely the functional antiviral factor in mouse cells (Oudshoorn and others 2012).

Here, we established the Herc6 null mice to study their role in protein ISGylation *in vivo*. Herc6 knockout mice lacked protein ISGylation. Herc6-deficient primary MEFs and bone marrow-derived macrophages (BMDM) lost the capacity to conjugate ISG15 to a broad group of proteins. These analyses with our newly generated Herc6 knockout mice confirmed the previous finding in the *in vitro* system that Herc6 is the major ISG15 E3 ligase in mice. Furthermore, we examined STAT1 phospharylation on IFN-β treatment, production of IFN-β and IL-6 after SV infection, or double-stranded RNA poly I:C treatment of WT and Herc6$^{-/-}$ BMDM. No significant difference was detected. In addition, the virus titers of VSV in WT and Herc6$^{-/-}$ MEFs were similar. These results indicate that Herc6-mediated protein ISGylation has no obvious effect on IFN signaling and antiviral activity against SV and VSV under current experimental conditions. As a critical different phenotype from ISG15 E1 Ube1L knockout mice that also lack protein ISGylation, male Herc6-deficient mice showed severe seminal vesicle hypertrophy. This finding suggests that Herc6 has a role in regulating sperm sac morphology, which is independent of protein ISGylation.

## Materials and Methods

### *Generation of Herc6 knockout mice*

The *Herc6* mutant mice (accession No. CDB0585K; www.cdb.riken.jp/arg/mutant%20mice%20list.html) were generated by gene targeting in TT2 embryonic stem (ES) cells (Yagi and others 1993), as previously described (www.cdb.riken.jp/arg/Methods.html). Two *Herc6* mutant mouse strains (line 1, #29 and line 2, #51) were established from independent homologous recombinant ES cells, and no difference in phenotype was apparent between them. In this study, all of the experiments were carried out with line 1 (#29) mice.

### *Animal studies*

CBA/C57BL6 Mix background Herc6 KO (4 times backcrossed) mice and C57BL6 pure background WT and Herc6 KO mice were maintained at Kobe BM laboratory (Oriental Bio Service, Inc.). C57BL6 pure background WT and UBE1L KO mice were maintained at UCSD Moores cancer center. Animal studies in Kobe BM laboratory were properly conducted in accordance with regulations regarding animal experiments in Japan. Animal experiments in UCSD Moores cancer center were performed in accordance with NIH policies on the use of laboratory animals and approved by the Animal Research Committee of the Office for the Protection of Research Subjects at the University of California, San Diego.

### *Southern blotting and PCR genotyping*

Southern blots were performed using a radioactive label or DIG label (Roche) methods according to the manufacturer's protocols. The probe for Southern blotting was amplified using primers as follows: Fw (5′-TGA AGACAG ACA AGG TGG AAT AAC TTG ATA-3′), Rev (5′-CAG CTG CAG TAC CAC AGG TGA TGT GGT ACT-3′). The genotyping of mice was routinely performed with tail by PCR using a mixture of 3 primers after overnight treatment with proteinase K in PCR buffer. The sizes of the PCR products are WT allele (258 bp) and mutant allele (787 bp). The PCR primers were as follows: P1 (5′-ACA GGA TGT GAT AGG CTG CAT GTG AAA G-3′) and P3 (5′-AAA CAC CTA GTT CCC GAG GCT GTG AAC T-3′) for the *Herc6* WT allele; P2 (5′-ATC AGG ATG ATC TGG ACG AAG AGC ATC A-3′) and P3 for the *Neo* gene. The PCR conditions were 95°C for 2 min, 40 cycles of 95°C for 30 s, 55°C for 30 s, and 72°C for 1 min, followed by 72°C for 10 min.

### *Cell culture and transfection*

MEFs were prepared from E12.5 embryos and grown in Dulbecco's modified Eagle medium supplemented with glutamine, penicillin/streptomycin, and 10% fetal bovine serum (FBS). BMDM were cultured in RPMI1640 medium supplemented with glutamine, penicillin/streptomycin, 10% FBS, and macrophage colony-stimulating factor. For the knockdown analysis, siRNA was transfected using Lipofectamine 2000 (Invitrogen) according to the manufacturer's instruction. At 72 h after the siRNA transfection, cell lysates were prepared for examination.

### *Antibodies and reagents*

Anti-mouse Herc6 polyclonal antibodies were generated in rabbits by using the mouse Herc6 recombinant protein that was bacterially produced using GST (6P-1) mHerc6 652-1003aa. Antibodies against STAT1, p-STAT1 (Y701), and ISG15 (#2743) were purchased from Cell Signaling. For the detection of protein ISGylation in liver and spleen tissue samples of WT and Herc6 knockout mice with or without poly I:C injection, and BMDM samples of WT and Herc6 knockout mice with or without IFN-β treatment, we used Dong-Er Zhang Lab's anti-mouse ISG15 antibody. Anti-α-tubulin (Sigma) and actin were acquired from Oncogene Research Products. Poly I:C was purchased from Amersham. Mouse IFN-β was purchased from PBL. Sendai virus (Z strain) and VSV were kindly provided by Dr. Masato Nakanishi (Research center for stem cell engineering, AIST, Japan).

### *Knockdown*

For knockdown of Herc6, the following siRNAs were used:

si-Herc6-1: 5′-gaaauaagcuuuaugccuauu-3′ (B-Bridge International, Inc.)

si-Herc6-2: 5′-ggaacaaaguuaaagaacauu-3′ (B-Bridge International, Inc.)

si-Herc6-3: 5′-ccuacagaaugaaggaauauu-3′ (B-Bridge International, Inc.)

Control siRNA (si-GFP); 5′-acuuguacagcucguccauuu-3′ (B-Bridge International, Inc.)

### *Western blotting*

Western blotting was conducted as previously described (Arimoto and others 2010). All samples were denatured in 1× sample buffer [50 mM Tris-HCl (pH 6.8), 2% sodium dodecyl sulfate (SDS), 2-mercaptethanol, 10% glycerol, and 1% bromophenol blue] for 5 min at 100°C. Cells were lysed in RIPA buffer composed of 25 mM Tris-HCl (pH 8.0), 150 mM NaCl, 1 mM EDTA, 1 mM dithiothreitol, 0.1% SDS, 1% Nonidet P-40, and 0.5% sodium deoxycholate. The cell lysates were centrifuged (10,000 *g*) at 4°C for 5 min. All lysis buffer in this study contains proteinase and phosphatase inhibitors (Roche). For the quantification, the Fujifilm Multi-gauge V3.0 was used.

### *Enzyme-linked immunosorbent assay*

Culture media were collected and analyzed for IFN-β and IL-6 production by using enzyme-linked immunosorbent assays (ELISAs). ELISA kits for mouse IFN-β and IL-6 were purchased from PBL Biomedical Laboratories.

### *TCID50 assay*

50% tissue culture infectious dose (TCID50) assay was conducted as previously described (Arimoto and others 2010). Approximate viral titers were calculated by TCID50 assay. Results of this assay are well in accordance with those of the general plaque assay. After 12 h VSV infection,

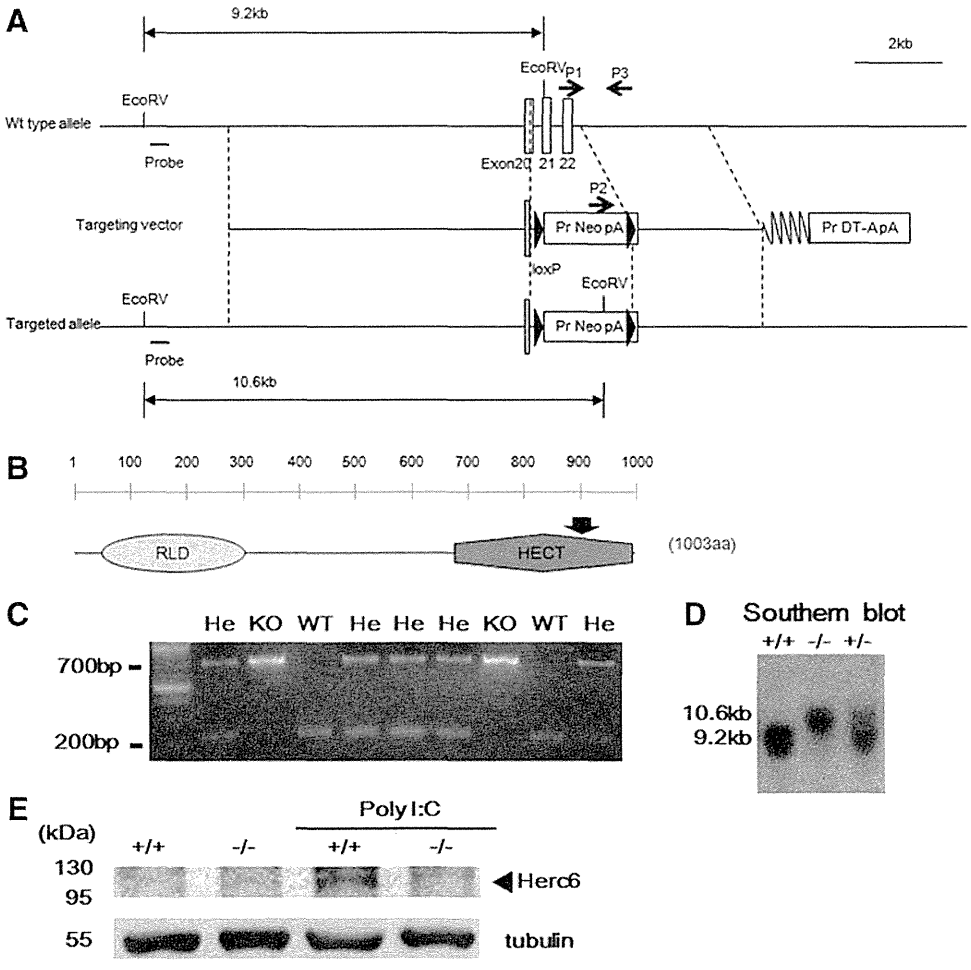


**FIG. 1.** Generation of Herc6 knockout mice. **(A)** Schematics of Herc6 knockout strategy. **(B)** Schematic diagram of Herc6 protein and the target deletion region is indicated with an *arrow*. **(C)** PCR genotyping of mouse tail DNA. **(D)** Southern blot analysis of mouse tail DNA. **(E)** Western blot analysis of protein ISGylation. Twenty-four hours after poly I:C injection, spleens were harvested. Herc6 protein was detected in the spleen extracts from WT mice, but not from Herc6 knockout mice by Western blotting using anti-mouse Herc6 polyclonal antibody. WT, wild type; He, heterozygous; KO, knockout.

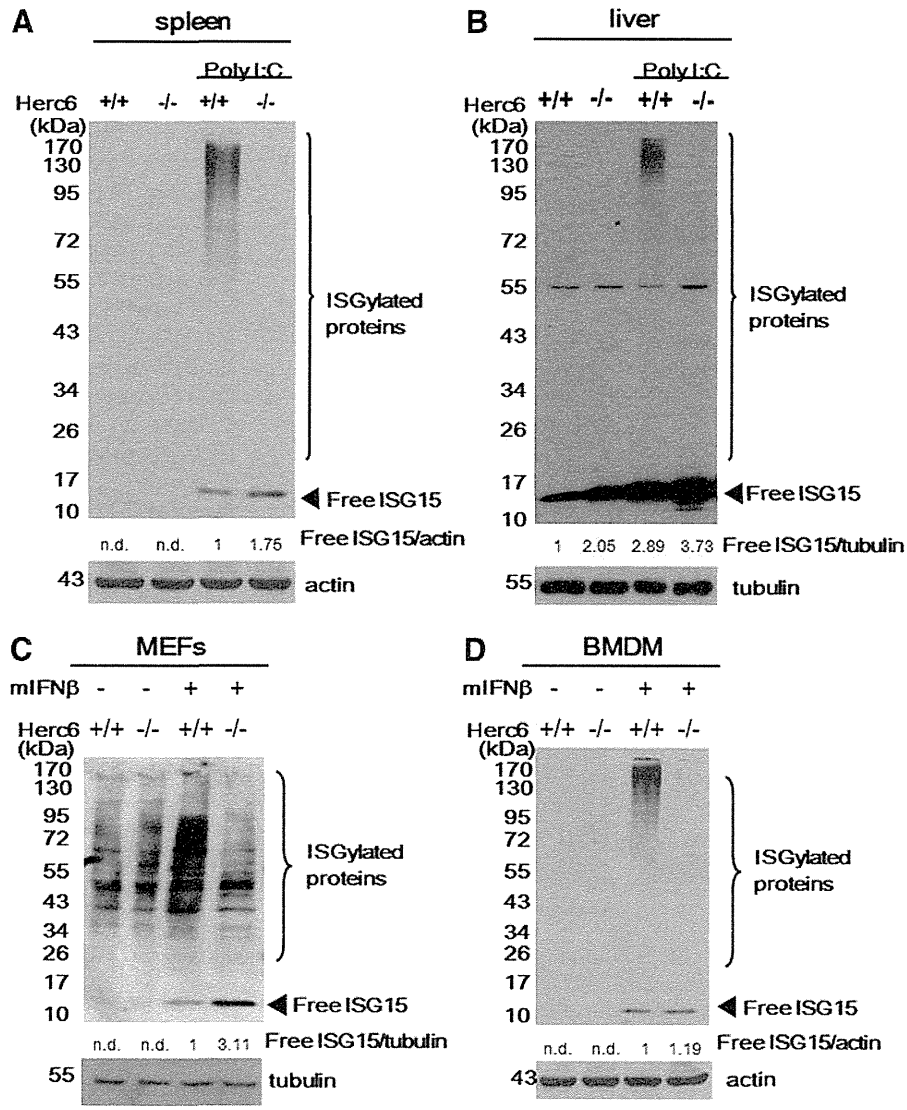


**FIG. 2.** Analysis of protein ISGylation in Herc6 knockout mice. **(A, B)** Twenty-four hours after PBS or poly I:C injection, spleens and livers were harvested, and ISG15 conjugated protein was detected by Western blotting using anti-mouse ISG15 antibody (Dong-Er Zhang Lab). **(C)** Mouse embryonic primary fibroblasts from WT and Herc6 knockout mice were treated with mock or 500 U/mL of mIFN-β. Twenty-four hours after treatment, cells were harvested and subjected to Western blotting using anti-ISG15 antibody (CST#2743), the information of which should be in M&M. **(D)** BMDM from wild-type and Herc6 knockout mice were treated with mock or 100 U/mL of mIFN-β as indicated. Twenty-four hours after treatment, cells were harvested and subjected to Western blotting using anti-mouse ISG15 antibody (Dong-Er Zhang Lab). The levels of free ISG15 were quantified as indicated. n.d. means not detectable. BMDM, bone marrow-derived macrophages; IFN, interferon.

the culture medium was diluted $3 \times 10^4$ times and then added to the first line of a 96-well plate with 50 μL medium containing 293T cells, making a serial 3-fold dilution. At 1–2 days after infection, more than 50% cell alterations in each dilution step was analyzed with the following formula: TCID50 = (rate of dilution at first line) × (dilution rate)$^{\Sigma-0.5}$, where Σ = the number of wells observed with more than 50% cell alteration in each dilution step/sample sum.

### *Histology*

Whole body was fixed by 10% formaldehyde solution, and tissues were paraffin embedded into OCT compound (Tissue-Tek). For histochemical analysis, paraffin sections were stained with H&E according to standard protocols.

## Results

### *Disruption of the mouse Herc6 gene*

In line with the previous report using L929 cells and siRNA against Herc6 (Oudshoorn and others 2012), we observed the reduction of ISGylation in Herc6 knockdown primary MEFs after IFN treatment (Supplementary Fig. S1; Supplementary Data are available online at www.liebertpub.com/jir). To investigate the role of protein ISGylation by Herc6 *in vivo*, we generated Herc6 knockout mice. For the disruption of the Herc6 gene, we added 2 *loxP* sites to exon 20 and the intron after exon 22 (Fig. 1A). This target region is related to C-terminal HECT domain of Herc6 protein (Fig. 1B). This construct also contains the bacterial neomycin gene as a selection marker in the Herc6 gene. Chimeric mice were produced by an injection of 2 independent clones of heterozygous ES cells into CBA blastocyst-stage embryos, and germ line transmission was determined by breeding with WT C57BL6 mice. We further backcrossed Herc6$^{+/-}$ mice with C57BL6 mice 4 times and 8 times to generate CBA/C57BL6 mix background and C57BL6 background Herc6 null mice, respectively. Mice were genotyped by PCR (Fig. 1C), and confirmed by Southern blot analysis (Fig. 1D). To confirm that Herc6 is no longer expressed in the knockout mice, spleens of WT and Herc6$^{-/-}$ mice that were with or without poly I:C injection were homogenized and subjected to Western blot. Herc6 protein was identified in poly I:C injected WT, but not in Herc6 knockout mouse (Fig. 1E).

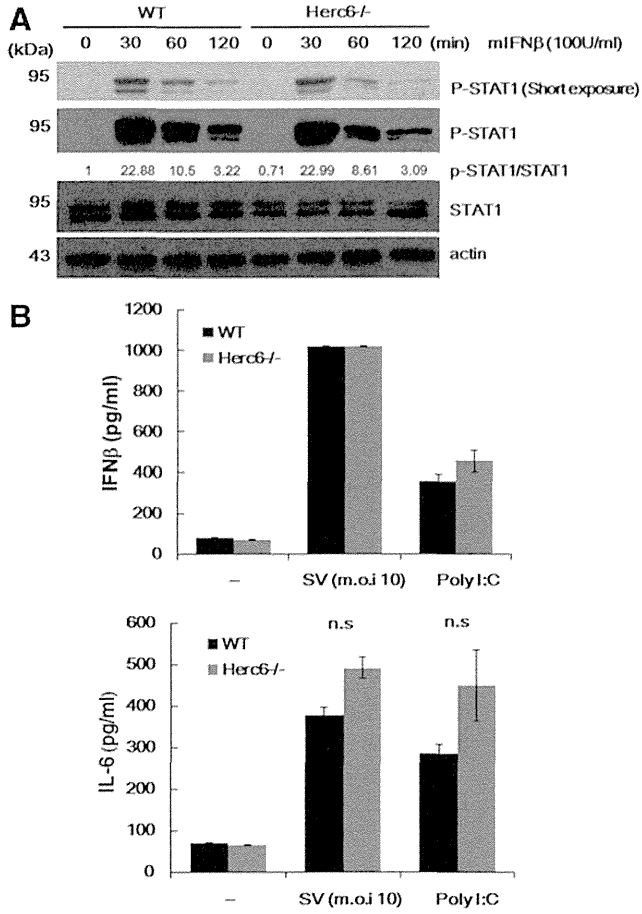


**FIG. 3.** Analysis of IFN and inflammatory response in Herc6 knockout cells. **(A)** BMDM from WT and Herc6 knockout mice were cultured in the presence of 100 U/mL of mIFN-β for the indicated time periods. Cells were harvested and subjected to Western blotting against pSTAT1, STAT1, and actin. The ratio of p-STAT1/total-STAT1 was also quantified as indicated. **(B)** Macrophages from WT and Herc6 knockout mice were treated with mock, SV at m.o.i. 10, or poly I:C 10 μg/mL. Twenty-four hours after treatment, cell culture media were harvested and subjected to ELISA for mIFN-β (*upper*) or mIL-6 (*bottom*). ELISA, enzyme-linked immunosorbent assay; m.o.i., multiplicity of infection; SV, Sendai virus.

### *Defective protein ISGylation in Herc6 knockout mice*

To determine whether lack of Herc6 correlated with decreased ISGylation *in vivo*, we injected WT and knockout mice with PBS or poly I:C. Twenty-four hours later, spleens and livers were harvested, and protein ISGylation was detected by Western blotting. Protein ISGylation was readily detected in the liver and spleen from WT but was barely detected from Herc6 knockout mice (Fig. 2A and B, respectively). Similar results were observed in IFN-β-treated MEFs and BMDM from WT and Herc6 knockout mice (Fig. 2C and D, respectively). Herc6-deficient tissues or cells showed an increased amount of free ISG15 as a result of the lack of conjugation (Fig. 2A–D).

These results indicate that Herc6 knockout mice are defective in protein ISGylation but not in free ISG15 expression.

### *Normal IFN responses of Herc6-deficient cells and mice*

A previous report has shown that human HERC5 positively regulates the IFN-β promoter via enhancing IRF3 function and so confers antiviral activity (Shi and others 2010). In addition, mouse Herc6 also enhanced IFN-β promoter activity similar to its human Herc5 counterpart (Oudshoorn and others 2012). To explore whether Herc6 regulates IFN signal transduction, we examined the IFN-response of Herc6-deficient cells. Macrophages derived from bone marrow cells of WT and Herc6 knockout mice were cultured *in vitro* and treated with 100 U/mL of IFN-β, and STAT1 phosphorylation was detected as an indication of the activation of the signaling pathway. Increased phosphorylation of STAT1 on IFN treatment was observed. However, there was no difference of STAT1 phosphorylation between WT and Herc6-deficient cells (Fig. 3A).

To investigate whether the mouse Herc6 enhances an innate immune signal, we examined the IFN-β and IL-6 production in WT and Herc6$^{-/-}$ MEFs on Sendai virus infection and poly I:C stimulation. No significant differences in WT and Herc6 cells were observed (Fig. 3B top and bottom, respectively). Although it was not significant, a modest increase of IL-6 production in Herc6$^{-/-}$ MEFs with SV infection or poly I:C stimulation was observed (Fig. 3B bottom). This should be investigated with greater detail in the future.

Since lipopolysaccharide (LPS) activates the expression of these genes via the IFN signaling pathway, we also examined the peripheral blood cell count and other blood parameters.

TABLE 1. BLOOD ANALYSIS WITH OR WITHOUT LPS (15 mg/kg BODY WEIGHT) INJECTION

| | *WBC* ($10^3/\mu L$) | *RBC* ($10^3/\mu L$) | *Hb (g/dL)* | *Ht (%)* | *MCV (fl)* | *MCH (pg/cell)* | *MCHC (g/dL)* | *PLT* ($10^3/\mu L$) |
|---|---|---|---|---|---|---|---|---|
| Mock | | | | | | | | |
| WT ($n=3$) | 7.7±1.4 | 8.0±0.2 | 12.3±0.1 | 38.6±1.2 | 48±0.2 | 15.4±0.3 | 32.0±0.8 | 107.9±34.7 |
| KO ($n=2$) | 6.5±0.3 | 6.8±0.2 | 12±0.9 | 32.9±8.2 | 48.2±2.4 | 18.1±4.3 | 37.3±7.2 | 118.9±13.4 |
| LPS | | | | | | | | |
| WT ($n=5$) | 3.0±0.5 | 8.1±0.2 | 12.7±0.1 | 39.9±1.3 | 48.9±0.4 | 15.8±0.3 | 31.9±0.7 | 346.0±10.2 |
| KO ($n=5$) | 3.6±0.8 | 8.1±0.4 | 13.0±0.8 | 40.8±2.1 | 50.1±0.3 | 16.0±0.3 | 31.8±0.7 | 301.0±9.51 |

Blood samples were collected via retro-orbital bleeding from wild-type and Herc6 knockout mice at 1 day after with or without LPS (15 mg/kg body weight) injections. Values are means±standard deviation.

WBC, white blood corpuscles; RBC, red blood corpuscles; Hb, hemoglobin; Ht, hematocrit; MCV, mean corpuscular volume; MCH, mean corpuscular hemoglobin; MCHC, mean corpuscular hemoglobin concentration; PLT, platelet; LPS, lipopolysaccharide; WT, wild type.

However, no significant differences were observed between WT and Herc6 knockout mice with or without LPS stimulation (Table 1).

In summary, Herc6-deficient cells do not show any detectable differences from WT cells in their responses to IFN-related treatments.

### *Deletion of Herc6 did not affect the antiviral response against VSV infection*

Besides the IFN response (Shi and others 2010), a recent report indicated that Herc5 mainly conjugates ISG15 to newly synthesized proteins in tissue culture and may by this mechanism largely target *de novo* synthesized viral proteins during infection (Durfee and others 2010).

To investigate whether Herc6 affects the proliferation of virus, we examined the consequences of reduction of protein ISGylation on the antiviral effects of IFN in MEFs. Treatment with increasing concentrations of IFN-β correlated positively with the antiviral stage of both WT and Herc6 knockout MEFs on infection with VSV, with no detectable differences in the response between the 2 genotypes (Fig. 4A). In addition, there was no significant difference of viral titer between WT and Herc6 knockout MEFs after infection with VSV (Fig. 4B). These experiments demonstrate that protein ISGylation via Herc6 in mice is not involved in the antiviral response against VSV.

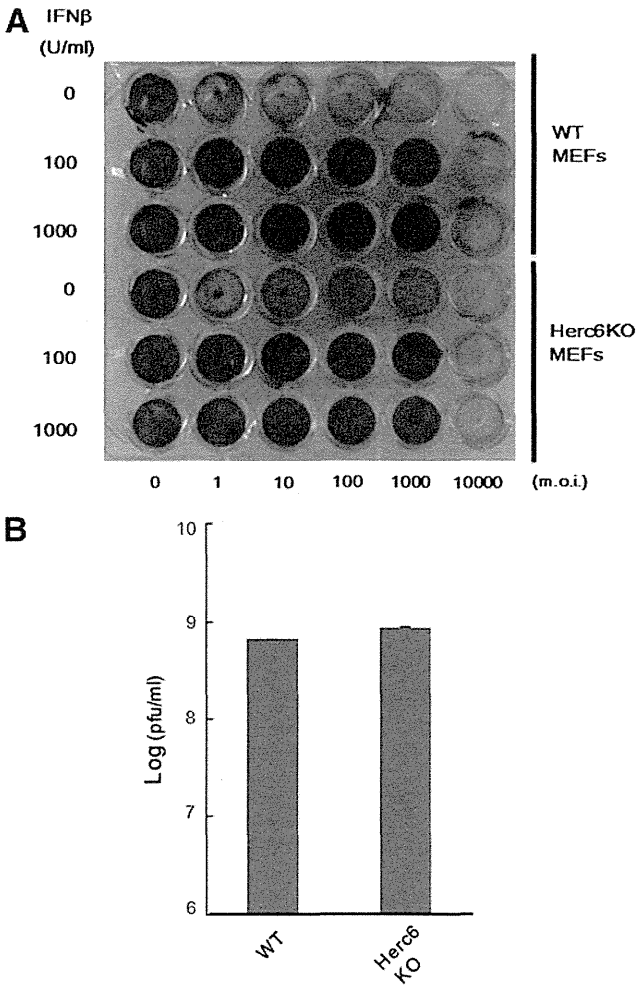


**FIG. 4.** VSV protection assay. **(A)** WT and Herc6 knockout MEFs were left untreated or treated with 100 or 1,000 U/mL of IFN-β for 24 h, followed by VSV infection at m.o.i. 0–$10^4$ per well for an additional 24 h. Cell viability was assessed by crystal *violet* staining. **(B)** The VSV (m.o.i. 0.1) was infected with WT and Herc6 knockout MEFs. At 12 h after infection, virus titer was measured according to TCID50 protocol. Data are mean ± SD ($n = 3$). MEFs, mouse embryonic fibroblast cells; TCID50, 50% tissue culture infectious dose; VSV, vesicular stomatitis virus.

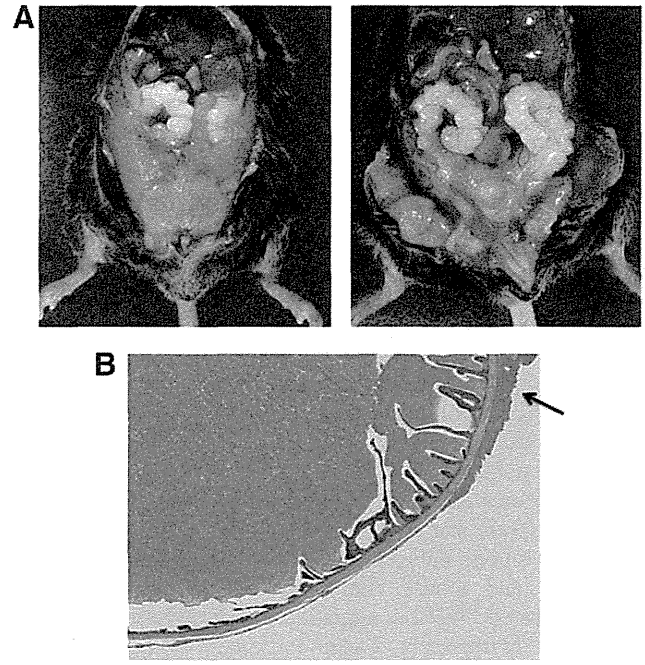


**FIG. 5.** The phenotype of Herc6 knockout mice. **(A)** The representative enlarged seminal vesicle in Herc6 knockout mouse (30 weeks, mix background). *Right panel* shows incision of the peritoneum of the left mouse. **(B)** H&E staining for the seminal vesicle of Herc6 knockout mouse. *Arrow* shows epithelial hyperplasia of seminal vesicle.

### *Male Herc6 null mice showed hypertrophy of seminal vesicle*

During the experiments, we noticed that mix-background Herc6 knockout male mice began showing abdominal distension at 28 weeks. Severe enlargement seminal vesicles were observed in Herc6 knockout mice (Fig. 5A). However, only slight epithelial hyperplasia with cystic dilatation of seminal vesicles was observed in Herc6 knockout mice (Fig. 5B), suggesting that the enlargement of seminal vesicles was from increased seminal fluid. Glandular hypoplasia and benign hypertrophy of the prostate, which are commonly found in elderly men, were not observed in Herc6 knockout mice (data not shown). Further examination using C57BL6 background mice showed a higher frequency of enlargement of seminal vesicles in Herc6 knockout mice compared with WT or UBE1L knockout mice (Table 2 and Supplementary Fig. S2). These results demonstrate that mouse Herc6 has an ISG15-independent function in regulating the seminal component.

## Discussion

In this article, we described the generation and analysis of the first Herc6 knockout mouse model. The results of our

TABLE 2. ANALYSIS OF SEMINAL VESICLE OF WT, UBE1L$^{-/-}$, AND HERC6$^{-/-}$, MICE

| *Background* | *Genotype* | *Population of hypertrophied seminal vesicle* | | |
|---|---|---|---|---|
| | | 30 weeks | 50 weeks | ~90 weeks |
| Mix (CBA/C57BL6) | Herc6$^{-/-}$ ($n=5$) | 2 | 4 | |
| C57 | WT ($n=10$) | | 0 | 2 |
| | UBE1L$^{-/-}$ ($n=5$) | | 0 | 0 |
| | Herc6$^{-/-}$ ($n=9$) | | 1[a] | 8 |

[a]One-side anomalistic seminal hypertrophy.
Seminal hypertrophy is defined as above at least 0.04 g seminal vesicle/g body weight.

studies demonstrate that (1) Mouse Herc6 is the major E3 ligase for ISG15 conjugation *in vivo*. (2) ISG15 conjugation via mouse Herc6 does not affect type I IFN response and antiviral response against SV and VSV infection. (3) Mouse Herc6 possesses an ISG15 conjugation-independent role in regulating sperm sac morphology.

Previous reports indicate that human Herc5 knockdown in 293T cells and mouse Herc6 knockdown in L929 cells showed reduced ISG15 conjugation to a broad group of proteins after IFN treatment (Dastur and others 2006; Wong and others 2006; Oudshoorn and others 2012). In line with this result, the level of ISG15 conjugation in tissues of Herc6-deficient mice showed substantial reduction compared with that of WT mice after poly I:C injection. These findings clearly indicate that Herc6 is the major mouse ISG15 E3 ligases *in vivo*. Furthermore, our report supports that humans and mice developed different Herc proteins to facilitate global ISG15 conjugation during evolution.

A recent report indicates that HERC5 is mainly associated with poly-ribosome, and ISGylation targets newly synthesized proteins in human tissue culture (Durfee and others 2010). Furthermore, in this same report, the authors showed that HPV16 L1 capsid protein was ISGylated and this modification inhibited HPV pseudovirus production in transfection experiments (Durfee and others 2010). In addition, previous reports showed that antiviral effects exerted by human HERC5 (Shi and others 2010) are shared by Herc6 in mouse cells (Oudshoorn and others 2012). ISG15-activating enzyme Ube1L knockout mice also showed no protein ISGylation and no difference in IFN responses and anti-VSV and LCMV defense (Osiak and others 2005; Kim and others 2006). However, further studies of Ube1L knockout mice revealed a critical role of Ube1L in control of influenza B virus infection (Lai and others 2009). These discrepancies of revealed functions of protein ISGylation are likely due to the differences in species (humans and mice), lines, and viruses, and *in vitro* versus *in vivo* experiments. These questions need to be addressed in the future.

Herc6 null mice showed hypertrophy of seminal vesicles in both CBA/C56BL6 mixed background and C57BL6 background. However, Ube1L$^{-/-}$ mice did not show similarly enlarged sperm sacs although protein ISGylation is lost in both Herc6 and Ube1L knockout mice (Kim and others 2006). This difference suggests that mouse Herc6 has an ISG15-independent function in seminal fluid production during aging. However, the phenotype of Herc6$^{-/-}$ ISG15$^{-/-}$ also should be investigated in the future to examine whether this seminal hypertrophy is truly Herc6 dependent and ISG15 independent. Since mouse Herc6 belongs to the Herc family of ubiquitin E3 ligases, it is possible that ISG15 conjugation is regulated by the ISG15 E3 ligase activity of Herc6, and seminal component secretion is regulated by its ubiquitin E3 ligase activity. Human Herc5 may have evolved to exclusively function as an ISG15 E3 ligase, while human Herc6 may function as a ubiquitin E3 ligase that is involved in the seminal component secretion.

While we could not see the difference in male fertility of Herc6 knockout mice (~35 weeks) (data not shown), we cannot rule out this possibility because it could be affected by the conditions associated with older age.

The function of seminal fluid is largely unknown except for the involvement of normal conception. Interestingly, it has recently been reported that paternal seminal fluid composition affects the epigenome of male offspring and that its impact on the periconception environment involves not only sperm protection but also indirect effects on various female factors regulating embryo development, which suggests that offspring of Herc6 null mice may have interesting epigenomic changes by the hypertrophied seminal vesicles of Herc6 male mice (Bromfield and others 2014). Future studies using this mouse model may facilitate to address this question.

In humans, symptoms of enlarged seminal vesicles are frequently seen in patients with ejaculatory duct obstructions (EDO) (Pryor and Hendry 1991). EDO is a congenital or acquired pathological condition that is characterized by the obstruction of one or both ejaculatory ducts, and causes 1%–5% of male infertility (Philip and others 2007). In addition to the congenital form that is often caused by cysts of the müllerian duct, the obstruction can be acquired due to an inflammation caused by chlamydia, prostatitis, tuberculosis of the prostate, and other pathogens (Philip and others 2007). However, in many patients, there is no history of inflammation and the underlying cause simply remains unknown (Philip and others 2007). The finding that the suppression of Herc6 caused the hypertrophied seminal vesicles in this report may be involved in the acquired enlarged seminal vesicle symptoms, and this should be investigated in the future.

## Acknowledgments

The authors thank all lab members for helpful discussion. They especially thank Dr. Kentson Lam (School of Medicine, University of California San Diego) and Samuel Stoner (Moores Cancer Center, University of California San Diego) for discussion and a critical reading of this article. They also thank Shuichiro Ogawa (Kyoto University) for several experiments and discussion. This study was supported by Grants-in-Aid for Scientific Research from the Ministry of Education, Culture, Sports, Science, and Technology (22114004 & 22249012), funding from National Institutes of Health USA (R01CA177305 and R01HL091549), and

JSPS KAKENHI Grant (No. 10J00577); Kei-ichiro Arimoto is a JSPS Postdoctoral Fellow for Research Abroad.

## Author Disclosure Statement

There is no financial interest to disclose.

## References

Arimoto K, Funami K, Saeki Y, Tanaka K, Okawa K, Takeuchi O, Akira S, Murakami Y, Shimotohno K. 2010. Polyubiquitin conjugation to NEMO by triparite motif protein 23 (TRIM23) is critical in antiviral defense. Proc Natl Acad Sci U S A 107(36):15856–15861.

Bedford L, Lowe J, Dick LR, Mayer RJ, Brownell JE. 2011. Ubiquitin-like protein conjugation and the ubiquitin-proteasome system as drug targets. Nature reviews. Drug Discov 10(1):29–46.

Bromfield JJ, Schjenken JE, Chin PY, Care AS, Jasper MJ, Robertson SA. 2014. Maternal tract factors contribute to paternal seminal fluid impact on metabolic phenotype in offspring. Proc Natl Acad Sci U S A 111(6):2200–2205.

Burkart C, Arimoto K, Tang T, Cong X, Xiao N, Liu YC, Kotenko SV, Ellies LG, Zhang DE. 2013. Usp18 deficient mammary epithelial cells create an antitumour environment driven by hypersensitivity to IFN-lambda and elevated secretion of Cxcl10. EMBO Mol Med 5(7):967–982.

Dastur A, Beaudenon S, Kelley M, Krug RM, Huibregtse JM. 2006. Herc5, an interferon-induced HECT E3 enzyme, is required for conjugation of ISG15 in human cells. J Biol Chem 281(7):4334–4338.

Durfee LA, Lyon N, Seo K, Huibregtse JM. 2010. The ISG15 conjugation system broadly targets newly synthesized proteins: implications for the antiviral function of ISG15. Mol Cell 38(5):722–732.

Guerra S, Caceres A, Knobeloch KP, Horak I, Esteban M. 2008. Vaccinia virus E3 protein prevents the antiviral action of ISG15. PLoS Pathog 4(7):e1000096.

Hochrainer K, Mayer H, Baranyi U, Binder B, Lipp J, Kroismayr R. 2005. The human HERC family of ubiquitin ligases: novel members, genomic organization, expression profiling, and evolutionary aspects. Genomics 85(2):153–164.

Hsiang TY, Zhao C, Krug RM. 2009. Interferon-induced ISG15 conjugation inhibits influenza A virus gene expression and replication in human cells. J Virol 83(12):5971–5977.

Hsiao NW, Chen JW, Yang TC, Orloff GM, Wu YY, Lai CH, Lan YC, Lin CW. 2010. ISG15 over-expression inhibits replication of the Japanese encephalitis virus in human medulloblastoma cells. Antiviral Res 85(3):504–511.

Kim KI, Giannakopoulos NV, Virgin HW, Zhang DE. 2004. Interferon-inducible ubiquitin E2, Ubc8, is a conjugating enzyme for protein ISGylation. Mol Cell Biol 24(21):9592–9600.

Kim KI, Yan M, Malakhova O, Luo JK, Shen MF, Zou W, de la Torre JC, Zhang DE. 2006. Ube1L and protein ISGylation are not essential for alpha/beta interferon signaling. Mol Cell Biol 26(2):472–479.

Lai C, Struckhoff JJ, Schneider J, Martinez-Sobrido L, Wolff T, Garcia-Sastre A, Zhang DE, Lenschow DJ. 2009. Mice lacking the ISG15 E1 enzyme UbE1L demonstrate increased susceptibility to both mouse-adapted and non-mouse-adapted influenza B virus infection. J Virol 83(2):1147–1151.

Lenschow DJ. 2010. Antiviral properties of ISG15. Viruses 2(10):2154–2168.

Lenschow DJ, Giannakopoulos NV, Gunn LJ, Johnston C, O'Guin AK, Schmidt RE, Levine B, Virgin HWt. 2005. Identification of interferon-stimulated gene 15 as an antiviral molecule during Sindbis virus infection *in vivo*. J Virol 79(22):13974–13983.

Lenschow DJ, Lai C, Frias-Staheli N, Giannakopoulos NV, Lutz A, Wolff T, Osiak A, Levine B, Schmidt RE, Garcia-Sastre A, Leib DA, Pekosz A, Knobeloch KP, Horak I, Virgin HWt. 2007. IFN-stimulated gene 15 functions as a critical antiviral molecule against influenza, herpes, and Sindbis viruses. Proc Natl Acad Sci U S A 104(4):1371–1376.

Malakhova OA, Zhang DE. 2008. ISG15 inhibits Nedd4 ubiquitin E3 activity and enhances the innate antiviral response. J Biol Chem 283(14):8783–8787.

Okumura A, Lu G, Pitha-Rowe I, Pitha PM. 2006. Innate antiviral response targets HIV-1 release by the induction of ubiquitin-like protein ISG15. Proc Natl Acad Sci U S A 103(5):1440–1445.

Okumura A, Pitha PM, Harty RN. 2008. ISG15 inhibits Ebola VP40 VLP budding in an L-domain-dependent manner by blocking Nedd4 ligase activity. Proc Natl Acad Sci U S A 105(10):3974–3979.

Osiak A, Utermohlen O, Niendorf S, Horak I, Knobeloch KP. 2005. ISG15, an interferon-stimulated ubiquitin-like protein, is not essential for STAT1 signaling and responses against vesicular stomatitis and lymphocytic choriomeningitis virus. Mol Cell Biol 25(15):6338–6345.

Oudshoorn D, van Boheemen S, Sanchez-Aparicio MT, Rajsbaum R, Garcia-Sastre A, Versteeg GA. 2012. HERC6 is the main E3 ligase for global ISG15 conjugation in mouse cells. PLoS One 7(1):e29870.

Park JM, Yang SW, Yu KR, Ka SH, Lee SW, Seol JH, Jeon YJ, Chung CH. 2014. Modification of PCNA by ISG15 plays a crucial role in termination of error-prone translesion DNA synthesis. Mol Cell 54(4):626–638.

Philip J, Manikandan R, Lamb GH, Desmond AD. 2007. Ejaculatory-duct calculus causing secondary obstruction and infertility. Fertil Steril 88(3):706 e9–e11.

Pincetic A, Kuang Z, Seo EJ, Leis J. 2010. The interferon-induced gene ISG15 blocks retrovirus release from cells late in the budding process. J Virol 84(9):4725–4736.

Pryor JP, Hendry WF. 1991. Ejaculatory duct obstruction in subfertile males: analysis of 87 patients. Fertil Steril 56(4):725–730.

Shi HX, Yang K, Liu X, Liu XY, Wei B, Shan YF, Zhu LH, Wang C. 2010. Positive regulation of interferon regulatory factor 3 activation by Herc5 via ISG15 modification. Mol Cell Biol 30(10):2424–2436.

Wong JJ, Pung YF, Sze NS, Chin KC. 2006. HERC5 is an IFN-induced HECT-type E3 protein ligase that mediates type I IFN-induced ISGylation of protein targets. Proc Natl Acad Sci U S A 103(28):10735–10740.

Yagi T, Tokunaga T, Furuta Y, Nada S, Yoshida M, Tsukada T, Saga Y, Takeda N, Ikawa Y, Aizawa S. 1993. A novel ES cell line, TT2, with high germline-differentiating potency. Anal Biochem 214(1):70–76.

Yuan W, Krug RM. 2001. Influenza B virus NS1 protein inhibits conjugation of the interferon (IFN)-induced ubiquitin-like ISG15 protein. EMBO J 20(3):362–371.

Address correspondence to:
*Dr. Kei-ichiro Arimoto*
*Moores UCSD Cancer Center*
*University of California, San Diego*
*3855 Health Sciences Drive*
*La Jolla, CA 92093*

*E-mail:* karimoto@ucsd.edu

Received 11 July 2014/Accepted 29 September 2014

THE JOURNAL OF BIOLOGICAL CHEMISTRY VOL. 290, NO. 9, pp. 5673–5684, February 27, 2015


# Dysregulation of Retinoic Acid Receptor Diminishes Hepatocyte Permissiveness to Hepatitis B Virus Infection through Modulation of Sodium Taurocholate Cotransporting Polypeptide (NTCP) Expression*

Received for publication, August 4, 2014, and in revised form, December 20, 2014 Published, JBC Papers in Press, December 30, 2014, DOI 10.1074/jbc.M114.602540

**Senko Tsukuda[‡§], Koichi Watashi[‡1], Masashi Iwamoto[‡], Ryosuke Suzuki[‡], Hideki Aizaki[‡], Maiko Okada[¶], Masaya Sugiyama[‖], Soichi Kojima[§], Yasuhito Tanaka[**], Masashi Mizokami[‖], Jisu Li[‡‡], Shuping Tong[‡‡], and Takaji Wakita[‡]**

*From the [‡]Department of Virology II, National Institute of Infectious Diseases, Tokyo 162-8640, Japan, the [§]Micro-signaling Regulation Technology Unit, RIKEN Center for Life Science Technologies, Wako 351-0198, Japan, the [¶]Department of Translational Oncology, St. Marianna University School of Medicine, Kawasaki 216-8511, Japan, the [‖]Research Center for Hepatitis and Immunology, National Center for Global Health and Medicine, Ichikawa 272-8516, Japan, the [**]Department of Virology and Liver Unit, Nagoya City University Graduate School of Medicinal Sciences, Nagoya 467-8601, Japan, and the [‡‡]Liver Research Center Rhode Island Hospital, Warren Alpert School of Medicine, Brown University, Providence, Rhode Island 02912*

**Background:** Host factors regulating hepatitis B virus (HBV) entry receptors are not well defined.
**Results:** Chemical screening identified that retinoic acid receptor (RAR) regulates sodium taurocholate cotransporting polypeptide (NTCP) expression and supports HBV infection.
**Conclusion:** RAR regulates NTCP expression and thereby supports HBV infection.
**Significance:** RAR regulation of NTCP can be a target for preventing HBV infection.

**Sodium taurocholate cotransporting polypeptide (NTCP) is an entry receptor for hepatitis B virus (HBV) and is regarded as one of the determinants that confer HBV permissiveness to host cells. However, how host factors regulate the ability of NTCP to support HBV infection is largely unknown. We aimed to identify the host signaling that regulated NTCP expression and thereby permissiveness to HBV. Here, a cell-based chemical screening method identified that Ro41-5253 decreased host susceptibility to HBV infection. Pretreatment with Ro41-5253 inhibited the viral entry process without affecting HBV replication. Intriguingly, Ro41-5253 reduced expression of both NTCP mRNA and protein. We found that retinoic acid receptor (RAR) regulated the promoter activity of the human *NTCP* (h*NTCP*) gene and that Ro41-5253 repressed the hNTCP promoter by antagonizing RAR. RAR recruited to the h*NTCP* promoter region, and nucleotides −112 to −96 of the h*NTCP* was suggested to be critical for RAR-mediated transcriptional activation. HBV susceptibility was decreased in pharmacologically RAR-inactivated cells. CD2665 showed a stronger anti-HBV potential and disrupted the spread of HBV infection that was achieved by continuous reproduction of the whole HBV life cycle. In addition, this mechanism was significant for drug development, as antagonization of RAR blocked infection of multiple HBV genotypes and also a clinically relevant HBV mutant that was resistant to nucleoside analogs. Thus, RAR is crucial for regulating NTCP expression that determines permissiveness to HBV infection. This is the first demonstration showing host regulation of NTCP to support HBV infection.**

Hepatitis B virus (HBV)[2] infection is a major public health problem, as the virus chronically infects ~240 million people worldwide (1–3). Chronic HBV infection elevates the risk for developing liver cirrhosis and hepatocellular carcinoma (4–6). Currently, two classes of antiviral agents are available to combat chronic HBV infection. First, interferon (IFN)-based drugs, including IFNα and pegylated-IFNα, modulate host immune function and/or directly inhibit HBV replication in hepatocytes (7, 8). However, the antiviral efficacy of IFN-based drugs is restricted to less than 40% (9, 10). Second, nucleos(t)ide analogs, including lamivudine (LMV), adefovir, entecavir (ETV), tenofovir, and telbivudine suppress HBV by inhibiting the viral reverse transcriptase (11, 12). Although they can provide significant clinical improvement, long term therapy with nucleos(t)ide analogs often results in the selection of drug-resistant mutations in the target gene, which limits the treatment outcome. For example, in patients treated with ETV, at least three mutations can arise in the reverse transcriptase sequence of the

* This work was supported in part by grants-in-aid from the Ministry of Health, Labor, and Welfare, Japan, from the Ministry of Education, Culture, Sports, Science, and Technology, Japan, and from Japan Society for the Promotion of Science, and by the incentive support from Liver Forum in Kyoto.
[1] To whom correspondence should be addressed: Dept. of Virology II, National Institute of Infectious Diseases, 1-23-1 Toyama, Shinjuku-ku, Tokyo, 162-8640, Japan. Tel.: 81-3-5285-1111; Fax: 81-3-5285-1161; E-mail: kwatashi@nih.go.jp.

[2] The abbreviations used are: HBV, hepatitis B virus; NTCP, sodium taurocholate cotransporting polypeptide; RAR, retinoic acid receptor; LMV, lamivudine; ETV, entecavir; HB, HBV surface protein; SLC10A1, solute carrier protein 10A1; hNTCP, human NTCP; ATRA, all-*trans*-retinoic acid; SHP, small heterodimer partner; ASBT, apical sodium-dependent bile salt transporter; RARE, RAR-responsive element; RXR, retinoid X receptor; SEAP, secreted alkaline phosphatase; FXR, farnesoid X receptor; MTT, 3-(4,5-dimethylthiazol-2-yl)-2,5-diphenyltetrazolium bromide; nt, nucleotide; cccDNA, covalently closed circular DNA.

polymerase L180M and M204V plus either one of Thr-184, Ser-202, or Met-250 codon changes to acquire drug resistance (13). Therefore, development of new anti-HBV agents targeting other molecules requires elucidation of the molecular mechanisms underlying the HBV life cycle.

HBV infection of hepatocytes involves multiple steps. The initial viral attachment to the host cell surface starts with a low affinity binding involving heparan sulfate proteoglycans, and the following viral entry is mediated by a specific interaction between HBV and its host receptor(s) (14). Recently, sodium taurocholate cotransporting polypeptide (NTCP) was reported as a functional receptor for HBV (15). NTCP interacts with HBV large surface protein (HBs) to mediate viral attachment and the subsequent entry step. NTCP, also known as solute carrier protein 10A1 (SLC10A1), is physiologically a sodium-dependent transporter for bile salts located on the basolateral membrane of hepatocytes (16). In the liver, hepatocytes take up bile salts from the portal blood and secrete them into bile for enterohepatic circulation, and NTCP-mediated uptake of bile salts into hepatocytes occurs largely in a sodium-dependent manner. Although NTCP is abundant in freshly isolated primary hepatocytes, it is weakly or no longer expressed in most cell lines such as HepG2 and Huh-7, and these cells rarely support HBV infection (17, 18). In contrast, primary human hepatocytes, primary tupaia hepatocyte, and differentiated HepaRG cells, which are susceptible to HBV infection, express significant levels of NTCP (19). Thus, elucidation of the regulatory mechanisms for *NTCP* gene expression is important for understanding the HBV susceptibility of host cells as well as for developing a new anti-HBV strategy. HBV entry inhibitors are expected to be useful for preventing *de novo* infection after liver transplantation, for post-exposure prophylaxis, or for vertical transmission by short term treatment (20, 21).

In this study, we used a HepaRG-based HBV infection system to screen for small molecules capable of decreasing HBV infection. We found that pretreatment of host cells with Ro41-5253 reduced HBV infection. Ro41-5253 reduced NTCP expression by repressing the promoter activity of the human *NTCP* (h*NTCP*) gene. Retinoic acid receptor (RAR) played a crucial role in regulating the promoter activity of h*NTCP*, and Ro41-5253 antagonized RAR to reduce *NTCP* transcription and consequently HBV infection. This and other RAR inhibitors showed anti-HBV activity against different genotypes and an HBV nucleoside analog-resistant mutant and moreover inhibited the spread of HBV. This study clarified one of the mechanisms for gene regulation of NTCP to support HBV permissiveness, and it also suggests a novel concept whereby manipulation of this regulation machinery can be useful for preventing HBV infection.

## EXPERIMENTAL PROCEDURES

*Reagents*—Heparin was obtained from Mochida Pharmaceutical. Lamivudine, cyclosporin A, all-*trans*-retinoic acid (ATRA), and TO901317 were obtained from Sigma. Entecavir was obtained from Santa Cruz Biotechnology. Ro41-5253 was obtained from Enzo Life Sciences. PreS1-lipopeptide and FITC-labeled preS1 were synthesized by CS Bio. IL-1$\beta$ was purchased from PeproTech. CD2665, BMS195614, BMS493, and MM11253 were purchased from Tocris Bioscience.

*Cell Culture*—HepaRG cells (BIOPREDIC) and primary human hepatocytes (Phoenixbio) were cultured as described previously (19). HepG2 and HepAD38 cells (kindly provided by Dr. Christoph Seeger at Fox Chase Cancer Center) (22) were cultured with DMEM/F-12 + GlutaMAX (Invitrogen) supplemented with 10 mM HEPES (Invitrogen), 200 units/ml penicillin, 200 $\mu$g/ml streptomycin, 10% FBS, and 5 $\mu$g/ml insulin. HuS-E/2 cells (kindly provided by Dr. Kunitada Shimotohno at National Center for Global Health and Medicine) were cultured as described previously (23).

*Plasmid Construction*—phNTCP-Gluc, pTK-Rluc was purchased from GeneCopoeia and Promega, respectively. pRARE-Fluc was generated as described (25). For constructing phNTCP-Gluc carrying a mutation in a putative RARE (nt −491 to −479), the DNA fragments were amplified by PCR using phNTCP-Gluc as a template with the following primer sets: F1, 5′-CAGATCTTGGAATTCCCAAAATC-3′ and 5′-GAGGGGATGTGTCCATTGAAATGTTAATGGGAGCT-GAGAGGATGCCAGTATCCTCCCT-3′ and primer sets 5′-CTCTCAGCTCCCATTAACATTTCAATGGACACATCC-CCTCCTGGAGGCCAGTGACATT-3′ and R6, 5′-CTCGGT-ACCAAGCTTTCCTTGTT-3′. The resultant products were further amplified by PCR with F1 and R6 and then inserted into the EcoRI/HindIII sites of phNTCP-Gluc to generate phNTCP Mut(−491 to −479)-Gluc. Other promoter mutants were prepared by the same method using the following primer sets: F1, 5′-GTGGGTTATCATTTGTTTCCCGAAAACATTAG-AGTGAAAGGAGCTGGGTGTTGCCTTTGG-3′ and 5′-TCCTTTCACTCTAATGTTTTCGGGAAACAAATGATA-ACCCACTGGACATGGGGAGGGCAC-3′; R6 for −368 to −356; F1 and 5′-AATCTAGGTCCAGCCTATTTAAGTCC-CTAAATTTCCTTTTCCCAGCTCCGCTCTTGATTCCTT-3′, 5′-CTGGGAAAAGGAAATTTAGGGACTTAAATAGG-CTGGACCTAGATTCAGGTGGGCCCTGGGCAG-3′, and R6 for −274 to −258; F1 and 5′-TTCTGGGCTTATTTCTA-TATTTTGCAATCCACTGAGTGTGCCTCATGGGCATT-CATTC-3′, 5′-CACACTCAGTGGATTGCAAAATATAGA-AATAAGCCCAGAAGCAGCAAAGTGACAAGGG-3′, and R6 for −179 to −167; F1 and 5′-AGCTCTCCCAAGCTCAA-AGATAAATGCTAGTTTCCTGGGTGCTACTTGTACTC-CTCCCTTGTC-3′, 5′-GTAGCACCCAGGAAACTAGCAT-TTATCTTTGAGCTTGGGAGAGCTAGGGCAGGCAGAT-AAGGT-3′, and R6 for −112 to −96, respectively. For constructing the hNTCP promoter carrying these five mutations (5-Mut), five DNA segments were amplified using the primers as follows: segment 1, F1 and 5′-GAGGGGATGTGTCCATG-ACC-3′; segment 2, 5′-AGCTCCTTTCACTCTCATGGGT-3′ and 5′-TCCTTTTCCCAGCTCCGC-3′; segment 3, 5′-GAG-CTGGGAAAAGGAGCTGC-3′ and 5′-CCACTGAGTGTG-CCTCATGG-3′; segment 4, 5′-AGGCACACTCAGTGGA-GGG-3′ and 5′-CTGGGTGCTACTTGTACTCCTCC-3′; and segment 5, 5′-CAAGTAGCACCCAGGAATCCA-3′ and R6. For producing a deletion construct for the h*NTCP* promoter, phNTCP (−53 to +108)-Gluc, DNA fragment was amplified using the primer sets 5′-GGTGAATTCTGTTCCTCTTTGG-GGCGACAGC-3′ and 5′-GGTGGTAAGCTTTCCTTGTTC-

TCCGGCTGACTCC-3′ and then inserted into the EcoRI and HindIII sites of phNTCP-Gluc.

*HBV Preparation and Infection*—HBV was prepared and infected as described (19). HBV used in this study was mainly derived from HepAD38 cells (22). For Fig. 8, *A–E*, we used concentrated (~200-fold) media of HepG2 cells transfected with an expression plasmid for either HBV genotypes A, B, C, D or genotype C carrying mutations at L180M, S202G, and M204V (HBV/Aeus, HBV/Bj35s, HBV/C-AT, HBV/D-IND60, or HBV/C-AT(L180M/S202G/M204V)) (24) and infected into the cells at 2000 GEq/cell in the presence of 4% PEG8000 at 37 °C for 16 h as described previously (19). HBV for Fig. 8*F* (genotype C) was purchased from Phoenixbio.

*Real Time PCR and RT-PCR*—Real time PCR for detecting HBV DNAs and cccDNA was performed as described (19). RT-PCR detection of mRNAs for *NTCP, ASBT, SHP*, and *GAPDH* was performed with one-step RNA PCR kit (TaKaRa) following the manufacturer's protocol with primer set 5′-AGGGAGGA-GGTGGCAATCAAGAGTGG-3′ and 5′-CCGGCTGAAGA-ACATTGAGGCACTGG-3′ for *NTCP*, 5′-GTTGGCCTTGG-TGATGTTCT-3′ and 5′-CGACCCAATAGGCCAAGATA-3′ for *ASBT*, 5′-CAGCTATGTGCACCTCATCG-3′ and 5′-CCA-GAAGGACTCCAGACAGC-3′ for *SHP*, and 5′-CCATGGAGA-AGGCTGGGG-3′ and 5′-CAAAGTTGTCATGGATGACC-3′ for *GAPDH*, respectively.

*Immunofluorescence Analysis*—Immunofluorescence was conducted essentially as described (25) using an anti-HBc antibody (DAKO, catalog no. B0586) at a dilution of 1:1000.

*Detection of HBs and HBe Antigens*—HBs and HBe antigens were detected by ELISA and chemiluminescence immunoassay, respectively, as described (19).

*MTT Assay*—The MTT cell viability assay was performed as described previously (19).

*Southern Blot Analysis*—Isolation of cellular DNA and Southern blot analysis to detect HBV DNAs were performed as described previously (19).

*Immunoblot Analysis*—Immunoblot analysis was performed as described previously (26, 27). Anti-NTCP (Abcam) (1:2000 dilution), anti-RARα (Santa Cruz Biotechnology) (1:6000 dilution), anti-RARβ (Sigma) (1:6000 dilution), anti-RARγ (Abcam) (1:2000 dilution), anti-RXRα (Santa Cruz Biotechnology) (1:8000 dilution), and anti-actin (Sigma) (1:5000 dilution) antibodies were used for primary antibodies.

*Flow Cytometry*—$1 \times 10^6$ primary human hepatocytes were incubated for 30 min with a 1:50 dilution of anti-NTCP antibody (Abcam) and then washed and incubated with a dye-labeled secondary antibody (Alexa Fluor 488, Invitrogen) at 1:500 dilution in the dark. Staining and washing were carried out at 4 °C in PBS supplemented with 0.5% bovine serum albumin and 0.1% sodium azide. The signals were analyzed with Cell Sorter SH8000 (Sony).

*FITC-preS1 Peptide-binding Assay*—Attachment of preS1 peptide with host cells was examined by preS1 binding assay essentially as described previously (28). HepaRG cells treated with or without Ro41-5253 (28) for 24 h or unlabeled preS1 peptide for 30 min were incubated with 40 nM FITC-labeled preS1 peptide (FITC-preS1) at 37 °C for 30 min. After washing the cells twice with culture medium and once with phosphate-buffered saline (PBS), the cells were fixed with 4% paraformaldehyde. Then the cells were treated with 4% Block Ace (DS Pharma Biomedical) containing DAPI for 30 min.

*Reporter Assay*—HuS-E/2 cells were transfected with phNTCP-Gluc (GeneCopoeia), a reporter plasmid carrying the *NTCP* promoter sequence upstream of the Gaussia luciferase (Gluc) gene, and pSEAP (GeneCopoeia), expressing the secreted alkaline phosphatase (SEAP) gene, together with or without expression plasmids for RARα, RARβ, RARγ, with RXRα using Lipofectamine 2000 (Invitrogen). At 24 h post-transfection, cells were stimulated with the indicated compounds for a further 24 h. The activities for Gluc as well as for SEAP were measured using a Secrete-Pair Dual-Luminescence assay kit (GeneCopoeia) according to the manufacturer's protocol, and Gluc values normalized by SEAP are shown.

pRARE-Fluc, carrying three tandem repeats of RAR-binding elements upstream of firefly luciferase (Fluc), and pTK-Rluc (Promega), which carries herpes simplex virus thymidine kinase promoter expressing *Renilla* luciferase (Rluc) (25), were used in dual-luciferase assays for detecting Fluc and Rluc. Fluc and Rluc were measured with Dual-Luciferase Reporter Assay System (Promega) according to the manufacturer's protocol, and Fluc activities normalized by Rluc are shown.

For evaluating HBV transcription in Fig. 2*B*, we used a reporter construct carrying HBV enhancer I, II, and core promoter (nt 1039–1788) ("Enh I + II") and that carrying enhancer II and core promoter (nt 1413–1788) ("Enh II"). These were constructed by inserting the corresponding sequences derived from a genotype D HBV in HepG2.2.15 cells into pGL4.28 vector (Promega). pGL3 promoter vector (Promega), which carries SV40 promoter ("SV40") was used as a control.

*Chromatin Immunoprecipitation (ChIP) Assay*—ChIP assay was performed using a Pierce-agarose ChIP kit (Thermo Fisher Scientific) according to the manufacturer's instructions. Huh7-25 cells transfected with phNTCP-Gluc together with or without expression plasmids for FLAG-tagged RARa and for RXRa were treated with 5 mg/ml actinomycin D for 2 h. The cells were then washed and treated with or without 2 mM ATRA for 60 min. Formaldehyde cross-linked cells were lysed, digested with micrococcal nuclease, and immunoprecipitated with anti-FLAG antibody (Sigma) or normal IgG. Input samples were also recovered without immunoprecipitation. DNA recovered from the immunoprecipitated or the input samples was amplified with primers 5′-CCCAGGGCCCACCTGAAT-CTA-3′ and 5′-TAGATTCAGGTGGGCCCTGGG-3′ for detection of NTCP.

## RESULTS

*Anti-HBV Activity of Ro41-5253*—We searched for small molecules capable of decreasing HBV infection in a cell-based chemical screening method using HBV-susceptible HepaRG cells (29). As a chemical library, we used a set of compounds for which bioactivity was already characterized (19). HepaRG cells were pretreated with compounds and then further incubated with HBV inoculum in the presence of compounds for 16 h (Fig. 1*A*). After removing free HBV and compounds by washing, the cells were cultured for an additional 12 days without compounds. For robust screening, HBV infection was monitored by

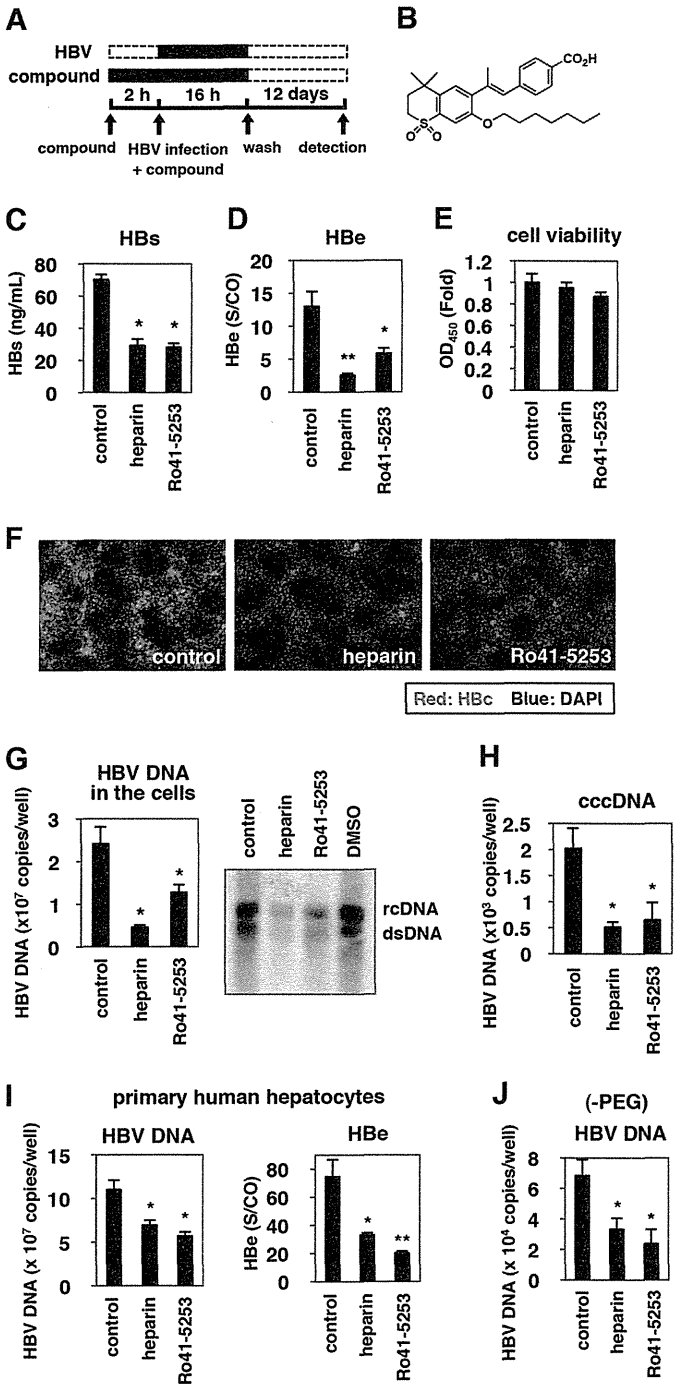


FIGURE 1. **Ro41-5253 decreased susceptibility to HBV infection.** *A*, schematic representation of the schedule for treatment of HepaRG cells with compounds and infection with HBV. HepaRG cells were pretreated with compounds for 2 h and then inoculated with HBV in the presence of compounds for 16 h. After washing out the free HBV and compounds, cells were cultured in the absence of compounds for an additional 12 days followed by quantification of secreted HBs protein. *Black* and *dashed bars* indicate the interval for treatment and without treatment, respectively. *B*, chemical structure of Ro41-5253. *C–E*, HepaRG cells were treated with or without 10 $\mu$M Ro41-5253 or 50 units/ml heparin according to the protocol shown in *A*, and HBs (*C*) and HBe (*D*) antigens in the culture supernatant were measured. Cell viability was also examined by MTT assay (*E*). *F–H*, HBc protein (*F*), HBV DNAs (*G*), and cccDNA (*H*) in the cells according to the protocol shown in *A* were detected by immunofluorescence, real time PCR, and Southern blot analysis. *Red* and *blue* in *F* show the detection of HBc protein and nuclear staining, respectively. *I* and *J*, primary human hepatocytes were treated with the indicated compounds and infected with HBV in the presence (*I*) or absence (*J*) of PEG8000 according to the protocol shown in *A*. The levels of HBV DNA in the cells (*I* and *J*) and HBe antigen in the culture supernatant (*I*) were quantified. The data show the means of three independent experiments. Standard deviations are also shown as *error bars*. Statistical significance was determined using Student's *t* test (*, $p < 0.05$; **, $p < 0.01$).

ELISA quantification of HBs antigen secreted from the infected cells at 12 days postinfection. This screening revealed that HBs was significantly reduced by treatment with Ro41-5253 (Fig. 1*B*) as well as heparin, a competitive viral attachment inhibitor that served as a positive control (Fig. 1*C*) (14). HBe in the medium (Fig. 1*D*) as well as intracellular HBc protein (Fig. 1*F*), HBV replicative (Fig. 1*G*), and cccDNA (Fig. 1*H*) were consistently decreased by treatment with Ro41-5253, without serious cytotoxicity (Fig. 1*E*). This effect of Ro41-5253 was not limited to infection of HepaRG cells because we observed a similar anti-HBV effect in primary human hepatocytes (Fig. 1*I*). The anti-HBV effect of Ro41-5253 on HBV infection of primary human hepatocytes was also observed in the absence of PEG8000 (Fig. 1*J*), which is frequently used to enhance HBV infectivity *in vitro* (14, 29). These data suggest that Ro41-5253 treatment decreases hepatocyte susceptibility to HBV infection.

*Reduced HBV Entry in Ro41-5253-treated Cells*—Ro41-5253 decreased HBs secretion from infected cells in a dose-dependent manner without significant cytotoxicity (Fig. 2*A*). We next investigated which step in the HBV life cycle was blocked by Ro41-5253. The HBV life cycle can be divided into two phases as follows: 1) the early phase of infection, including attachment, internalization, nuclear import, and cccDNA formation, and 2) the following late phase representing HBV replication that includes transcription, pregenomic RNA encapsidation, reverse transcription, envelopment, and virus release (19, 20, 30–34). LMV and ETV, inhibitors of reverse transcriptase, dramatically decreased HBV DNA in HepAD38 cells (Fig. 2*B*, *left panel*), which can replicate HBV DNA but are resistant to infection (22). However, LMV and ETV did not show a significant effect in HepaRG-based infection (Fig. 1*A*), in contrast to the anti-HBV effect of CsA, an HBV entry inhibitor (Fig. 2*C*) (19, 35), suggesting that this infection assay could be used to evaluate the early phase of infection without the replication process, including the reverse transcription. Ro41-5253 was suggested to inhibit the early phase of infection prior to genome replication as an anti-HBV activity was evident in Fig. 2*C* but not in Fig. 2*B*. Moreover, Ro41-5253 had little effect on HBV transcription, which was monitored by a luciferase activity driven from the HBV enhancer I, II, and the core promoter (Fig. 2*B*, *middle panel*), and by the HBV RNA level in HepG2.2.15 cells, persistently producing HBV (Fig. 2*B*, *right panel*) (36). We then examined whether Ro41-5253 pretreatment affected viral attachment to host cells. To this end, HepaRG cells were exposed to HBV at 4 °C for 3 h, which allowed HBV attachment but not subsequent internalization (19) (Fig. 2*D*). After washing out free viruses, cell surface HBV DNA was extracted and quantified to evaluate HBV cell attachment (Fig. 2*D*). Pretreatment with Ro41-5253 significantly reduced HBV DNA attached to the cell surface, as did heparin (Fig. 2*D*). In a preS1 binding assay, where FITC-labeled preS1 lipopeptide was used as a marker for HBV attachment to the cell surface, Ro41-5253-

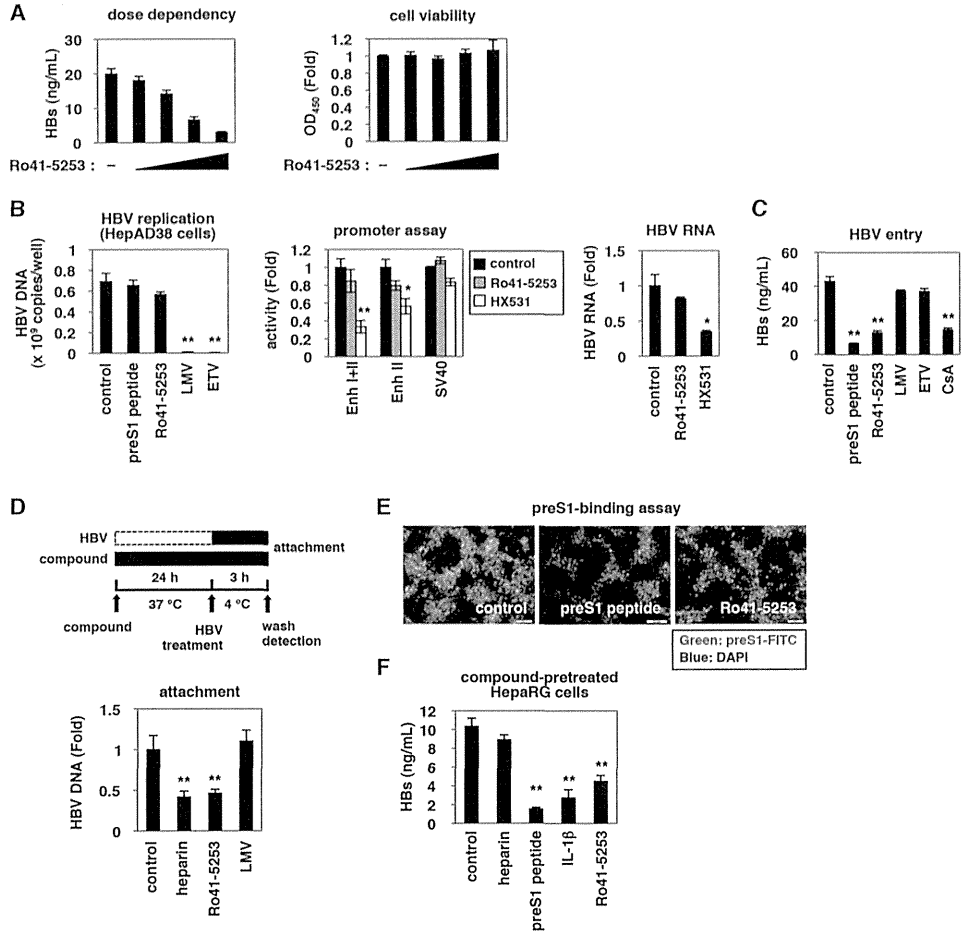


FIGURE 2. **Ro41-5253 decreased HBV entry.** *A*, HepaRG cells were treated with or without various concentrations (2.5, 5, 10, and 20 $\mu$M) of Ro41-5253 followed by HBV infection according to the protocol shown in Fig. 1*A*. Secreted HBs was detected by ELISA (*left panel*). Cell viability was also determined by ELISA (*right panel*). *B, left panel,* nucleocapsid-associated HBV DNA in HepAD38 cells treated with the indicated compounds (200 nM preS1 peptide, 20 $\mu$M Ro41-5253, 1 $\mu$M lamivudine, or 1 $\mu$M entecavir) for 6 days without tetracycline was quantified by real time PCR. *Middle panel,* HepG2 cells transfected with the reporter plasmids carrying HBV Enhancer (*Enh*) I + II, HBV Enhancer II, or SV40 promoter ("Experimental Procedures") were treated with or without Ro41-5253 or HX531 as a positive control to measure the luciferase activity. *Right panel,* HepG2.2.15 cells were treated with or without Ro41-5253 or HX531 for 6 days, and intracellular HBV RNA was quantified by real time RT-PCR. *C,* HepaRG cells were treated with or without indicated compounds (200 nM preS1 peptide, 20 $\mu$M Ro41-5253, 1 $\mu$M lamivudine, 1 $\mu$M entecavir, or 4 $\mu$M CsA) followed by HBV infection according to the protocol shown in Fig. 1*A*. *D, upper scheme* shows the experimental procedure for examining cell surface-bound HBV. The cells were pretreated with compounds (50 units/ml heparin, 20 $\mu$M Ro41-5253, or 1 $\mu$M lamivudine) at 37 °C for 24 h and then treated with HBV at 4 °C for 3 h to allow HBV attachment but not internalization into the cells. After removing free virus, cell surface HBV DNA was extracted and quantified by real time PCR. *E,* HepaRG cells pretreated with the indicated compounds (1 $\mu$M unconjugated preS1 peptide, 20 $\mu$M Ro41-5253) for 24 h were treated with 40 nM FITC-conjugated pre-S1 peptide (*FITC-preS1*) in the presence of compounds at 37 °C for 30 min. *Green* and *blue signals* show FITC-preS1 and nuclear staining, respectively. *F,* HepaRG cells pretreated with the indicated compounds (50 units/ml heparin, 200 nM preS1 peptide, 100 ng/ml IL-1$\beta$, or 20 $\mu$M Ro41-5253) for 24 h were used for the HBV infection assay, where HBV was inoculated for 16 h in the absence of the compounds. Statistical significance was determined using Student's *t* test (*, $p < 0.05$, and **, $p < 0.01$).

treated cells showed a reduced FITC fluorescence measuring viral attachment (Fig. 2*E*). Thus, Ro41-5253 primarily decreased the entry step, especially viral attachment. Next, to examine whether Ro41-5253 targeted HBV particles or host cells, HepaRG cells pretreated with compounds were examined for susceptibility to HBV infection in the absence of compounds (Fig. 2*F*). As a positive control, HBV infection was blocked by pretreatment of cells with an NTCP-binding lipopeptide, preS1(2–48)$^{myr}$ (preS1 peptide) (15), but not by heparin, which binds HBV particles instead (Fig. 2*F*, *2nd* and *3rd lanes*) (14). HBV infection was also diminished in HepaRG cells pretreated with IL-1$\beta$, which induced an innate immune response (Fig. 2*F*, *4th lane*) (37). In this experiment, Ro41-5253-pretreated HepaRG cells were less susceptible to HBV infection (Fig. 2*F*, *5th lane*), suggesting that the activity of Ro41-5253 in host cells contributed to the inhibition of HBV entry.

*Ro41-5253 Down-regulated NTCP*—Next, we examined how treatment of hepatocytes with Ro41-5253 decreased HBV susceptibility. Recently, NTCP was reported to be essential for HBV entry (15). Intriguingly, we found that Ro41-5253 decreased the level of NTCP protein in HepaRG cells (Fig. 3*A*). Flow cytometry showed that NTCP protein on the cell surface was consistently down-regulated following treatment with Ro41-5253 (Fig. 3*B*, compare *red* and *blue*). Semi-quantitative RT-PCR revealed that mRNA levels for *NTCP*, but not apical sodium-dependent bile salt transporter (ASBT, also known as NTCP2 or SLC10A2), another SLC10 family transporter, were reduced by Ro41-5253 in HepaRG cells (Fig. 3*C*). Thus, Ro41-5253 could reduce NTCP expression. When endogenous NTCP and RAR was knocked down by siRNA, the anti-HBV effect of Ro41-5253 was significantly diminished (Fig. 3*D*), suggesting that the inhibitory activity of Ro41-5253 to HBV infec-